

Evaluation of the southerly low-level jet climatology for the central United States as simulated by NARCCAP regional climate models

Ying Tang, Shiyuan Zhong, Julie A. Winker, Claudia K. Walters

Author Manuscript

This is the author manuscript accepted for publication and has undergone full peer review but has not been through the copyediting, typesetting, pagination and proofreading process, which may lead to differences between this version and the [Version of Record](#). Please cite this article as doi: [10.1002/joc.4636](https://doi.org/10.1002/joc.4636)

Abstract

An ensemble of simulations from four regional climate models (RCMs) driven by a global reanalysis was obtained from the North American Regional Climate Change Assessment Program (NARCCAP) and used to evaluate the ability of the RCMs to simulate the long-term (1979-2000) climatology of southerly low level jets (S-LLJs) in the central United States. The RCM-derived S-LLJ climatologies were evaluated against rawinsonde observations for the same period. The use of a small ensemble of RCM simulations helped to identify model differences and assisted with interpretation. The RCMs generally reproduced the broad spatial patterns and temporal variations of jet frequency and average jet height and speed. No model consistently outperformed the others in all aspects of the evaluation, although differences existed between models in the placement, migration and relative strength of "hotspots" of more frequent jet activity. In particular, three of the four models placed the center of greatest nocturnal S-LLJ activity during the warm season in northern and central Texas, whereas for the other model the greatest jet activity was located in the south-central plains (Kansas/Oklahoma). The magnitude of a S-LLJ frequency maximum over south Texas also varied between models, with simulated frequencies exceeding observed frequencies for some models but substantially underestimating for others. The evaluation presented here highlights the potential applications of RCMs in S-LLJ research for future climate and other assessment

studies that require three-dimensional data with relatively high spatial and temporal resolutions. The overall performance of the models in reproducing the long-term S-LLJ climatology supports the use of NARCCAP RCM simulations in climate assessments for the central United States where S-LLJs are an important contributor to the regional climatology.

Keywords: low level jet; regional climate models; model ensembles; NARCCAP; rawinsonde; climatology; evaluation

Author Manuscript

1. Introduction

A low level jet (LLJ) is a wind maximum in the lower troposphere. Although LLJs have been observed around the world, the central United States is particularly prone to frequent occurrences of LLJs, especially jets from a southerly direction (e.g., Bonner, 1968; Walters *et al.*, 2008). Southerly LLJs (S-LLJs) in this region transport warm, moist air from the Gulf of Mexico northward (Means, 1954; Helfand and Schubert, 1995), and have been related to nighttime precipitation maxima (Pitchford and London, 1962; Bonner, 1966). Because of the high wind speeds and strong wind shear associated with S-LLJs, their influence extends beyond weather and climate to include air pollution transport and dispersion (Banta *et al.*, 2002), forest fires (Charney *et al.*, 2003), transportation safety (Sjostedt *et al.*, 1990), insect outbreaks (Song *et al.*, 2005; Stensrud, 1996) and wind energy (Storm *et al.*, 2009).

The characteristics of S-LLJs in the central United States have been examined using observational data and numerical models. Most observational studies employed data from rawinsonde networks, although a few have used data from various other sources, including the National Oceanic and Atmospheric Administration (NOAA) profiler network (Mitchell *et al.*, 1995) and the National Centers for Environmental Prediction (NCEP) and the National Center for Atmospheric Research (NCAR) reanalyses

(Anderson and Arritt, 2001). Bonner's (1968) analysis of two years of twice-daily wind data from 47 rawinsonde stations across the United States provided the first comprehensive jet climatology and laid the foundation for future studies. Mitchell *et al.* (1995) developed a warm-season S-LLJ climatology at a higher temporal resolution using hourly wind profiler observations over the central Great Plains for 1991 and 1992. Whiteman *et al.* (1997) analyzed high vertical and temporal resolution rawinsonde observations for two years from a site in north-central Oklahoma, which provided a detailed climatology of S-LLJs in the southern Great Plains, whereas Song *et al.* (2005) analyzed jet occurrences for a site in Kansas based on hourly, high-resolution vertical profiles of wind velocity from a combination of a mini-sodar and a wind profiler. Although these studies significantly advanced our understanding of the vertical structure and evolution of S-LLJs, they were limited in space and time by relying on data from either a handful of stations or for short periods of time (one month to two years). In contrast, Walters *et al.* (2008), using a 40-year time series of wind observations from the rawinsonde network, provided a long-term climatology of jet frequency, direction, speed and elevation for the central United States although at a relatively coarse (~300 km) spatial scale.

Gridded reanalysis data have also been used to understand the climatological properties of S-LLJs. Doubler *et al.* (2015) developed a jet climatology for North

America and coastal environs using the North American Regional Reanalysis (NARR, Mesinger *et al.*, 2006) with 3-hourly output and 32 km resolution, and evaluated jet characteristics such as frequency, speed and elevation against prior sounding-based studies. They found strong agreement with existing climatologies and provided additional insights on the spatial extent and seasonal shifts of jet occurrences, for example, the involvement of a distinctive hotspot of enhanced frequencies in Texas. Walters *et al.* (2014) compared S-LLJs identified from NARR and rawinsonde wind profiles for 12 stations in the central United States for four representative years and found general agreement between the two data sources, although jet frequencies are smaller for NARR at most locations.

General circulation models (GCMs) have also been used to study the S-LLJ climatology over the central United States. For example, Helfand and Schubert (1995) employed a GCM to simulate Great Plains S-LLJs and their contribution to the water budget for two springtime months. The simulations highlighted the key role of S-LLJs in moisture transport in the central United States. Ghan *et al.* (1996) studied S-LLJs using two GCMs, and found that jets were generally well simulated despite the differences between models, although both models failed to simulate the physical connection between clouds and S-LLJs. Cook *et al.* (2008) examined simulations of S-LLJs over the Great Plains from 18 atmosphere-ocean GCMs during the 21st century and projected

more intense Great Plains S-LLJs during April, May, and June. As illustrated by these studies, an advantage of using GCM simulations to investigate S-LLJs is the greater spatial and temporal coverage compared to observational data. The relatively coarse spatial resolution (1 degree latitude or longitude), on the other hand, is a disadvantage. Other limitations include simulated S-LLJs that are either too weak or too strong, misplacement of the frequency maximum, or weak association with physical processes (Cook *et al.*, 2008; Ghan *et al.*, 1996).

Because a LLJ is a regional phenomenon, the use of regional climate model (RCM) outputs is likely to provide “added value” to the GCM-based studies by better resolving features important for S-LLJ formation such as terrain heterogeneity (the Rocky Mountains and the High Plains), coastlines (the Gulf of Mexico) and nocturnal surface-based inversions. RCMs primarily have been used to simulate an individual S-LLJ event (Zhong *et al.*, 1996; Storm *et al.*, 2009) or a series of jet events during a short time period, usually a few weeks or less (Werth *et al.*, 2011; Vanderwende *et al.*, 2015). Rarely have regional models been used to explicitly study the climatology of S-LLJs, although S-LLJs often appear in the results of regional climate simulations that were focused on a different phenomenon or processes in the central United States.

Because of the important role S-LLJs play in a variety of atmospheric processes, the ability of RCMs in simulating the vertical structure and the spatial and temporal

variability of S-LLJs needs to be evaluated before RCMs can be applied to understand these processes. To date, there has not been a systematic evaluation based on multiple models of how well RCMs simulate the S-LLJ climatology of the central United States. As mesoscale convective complexes frequently occur downstream of the jet nose, S-LLJs play a significant role in the formation of nocturnal precipitation in the Great Plains (Cook et al., 2008). RCM representations of S-LLJs often are only broadly compared with observations, usually with the goal of seeking possible factors contributing to biases in simulated regional precipitation (e.g., Liang *et al.*, 2004) rather than as an evaluation of a climatological phenomenon that merits its own in-depth assessment.

In this study, we aim to compare RCM results against sounding observations to provide an initial evaluation of how well RCMs simulate the long-term S-LLJ climatology of the central United States. Understanding the ability of RCMs to simulate S-LLJs under the current climate is critical for interpreting results from RCM future climate simulations and assessing the impact of climate change on S-LLJs. In order to examine the usefulness of RCM results, the spatial patterns of the characteristics (frequency, height, and speed) of S-LLJs are analyzed for a suite of four RCM simulations that were driven by the NCEP-Department of Energy (DOE) Reanalysis2 (referred to below as NCEP, Kanamitsu *et al.*, 2002) for the current climate and produced for the North American Regional Climate Change Assessment Project (NARCCAP,

Mearns *et al.*, 2012). This suite of RCM simulations was selected because of the wide use of the NARCCAP output in impacts studies as evidenced by over 100 published papers and reports (Mearns *et al.*, 2015), including many for the central United States (e.g., Takle *et al.*, 2010; Zhang *et al.*, 2011; Li *et al.*, 2012; Qiao *et al.*, 2014).

The specific objectives of the current study are to 1) examine the S-LLJ climatology simulated by the NARCCAP RCMs driven by the NCEP reanalysis for the current climate and 2) compare the simulated climatology with that of rawinsonde observations. The analyses will focus on the spatial distribution and diurnal, seasonal and annual variations of S-LLJs. As mentioned above, previous S-LLJ climatologies are limited either by the number of stations used in the analysis, the coarse resolution of the observing networks or GCM simulations, and/or the length of the study period. Regional climate models (RCMs) may act as a viable alternative for S-LLJ studies. The detailed S-LLJ climatology produced by a RCM ensemble, when evaluated against observations for an extended period, will significantly enhance our understanding of finer-scale spatial and temporal variations of S-LLJ characteristics and their representation in regional climate models.

2. Data and Methods

The most commonly-used definition of a LLJ was introduced by Bonner (1968), who defined a LLJ as a wind maximum $\geq 12 \text{ ms}^{-1}$ at or below 1.5 km above ground level (AGL), with a decrease by at least 6 ms^{-1} to the next higher minimum or 3 km AGL, whichever was lower. In the current study, the height range for the wind maxima is extended to 3 km and the height of the next higher minimum is extended to 5 km to account for synoptically-driven S-LLJs that often slope upward with latitude (Uccellini and Johnson, 1979). Following Walters *et al.* (2008), an additional criterion of a decrease below the jet nose of at least 6 ms^{-1} is prescribed. S-LLJs are limited to those jets with a direction between 113° - 247° . The S-LLJ climatology is generated from model simulations provided by the North American Regional Climate Change Assessment Program (NARCCAP) (Mearns *et al.*, 2007; Mearns *et al.*, 2009; Mearns *et al.*, 2012). NARCCAP is an international collaboration aiming to provide high resolution climate change scenarios for use in impacts research. Climate simulations were performed using a suite of RCMs driven by a set of GCMs for North America for both the current climate period 1971-2000 and the future climate period 2041-2070 (forced by the A2 scenario) (Mearns *et al.*, 2007; Mearns *et al.*, 2009). This study analyzes the set of RCM simulations driven by the NCEP reanalysis for the period 1979-2004. A 50 km horizontal grid spacing was used in all the RCM simulations. The archived data contains 28 vertical levels from 1050 hPa to 50 hPa, with a vertical resolution of 25 hPa below 700 hPa and 50 hPa above 700

hPa. Three-hourly data are available for NARCCAP outputs.

Four model runs are included in the current study, namely the Canadian Regional Climate Model (CRCM) (Laprise *et al.*, 1998; Caya and Laprise, 1999), the Weather Research and Forecasting model, updated Grell configuration (WRFG) (Skamarock *et al.*, 2005; Grell and Devenyi, 2002), the Regional Climate Model version 3 (RCM3) (Pal *et al.*, 2007), and the Hadley Regional Model 3 (HRM3) (Jones *et al.*, 2004). The other two RCMs in the NARCCAP suite, the Scripps Experimental Climate Prediction Center Regional Spectral Model and the fifth-generational Pennsylvania State University-National Center for Atmospheric Research Mesoscale Model are not included in the analysis because wind data at multiple vertical levels was not archived for these models. S-LLJs are extracted from the simulated vertical wind profiles based on the criteria described above.

The RCM-simulated S-LLJ climatology is compared to a sounding-based S-LLJ climatology as described in Walters *et al.* (2008) that was derived from a network of 36 rawinsonde stations across the central United States. A major limitation of the routine rawinsonde sounding data is that they are only twice per day, which is inadequate for capturing detailed diurnal variations. This limitation is overcome by radar wind profilers that provide hourly observations of vertical wind profiles. Data from wind profilers, however, are often limited by time span, region coverage, or data quality issues (Doubler

et al., 2015; Walters *et al.*, 2014). For example, the NOAA 404 MHz profiler has its lowest range gate around 500 m above ground which is not suitable for S-LLJ studies (Whiteman *et al.*, 1997). Although the 915 MHz profiler has its lowest range gate around 100 m above ground, measurements are confined to a few locations and for short periods and, consequently, are unsuitable for a climatological analysis (Whiteman *et al.*, 1997).

The simulated and observed climatologies are produced for the 21-year period, October 1979 - September 2000, which is the period of overlap between the RCM simulations and the database of jet occurrences developed by Walters *et al.* (2008). The locations of the rawinsonde stations along with the station elevations are shown in Figure 1. Also shown in Figure 1 is the representative topography as resolved by one of the RCMs. There are only small variations in topography across the four models, because the same horizontal grid spacing was adopted for all the NARCCAP simulations. The difference between the model topography and the station topography is relatively small for most stations except for a few near the western border of the rawinsonde network where the 50-km model grid spacing is too coarse to resolve the mountainous terrain.

To compare with the twice-daily soundings, only 00 UTC and 12 UTC are considered for the RCM data analysis. At either 00 or 12 UTC, jet frequency and average jet speed and height are calculated for each month of the year to enable an examination of sub-seasonal variations. The results are further grouped into warm (April – September)

and cold (October – March) seasons for the analysis of seasonal variability. The jet frequency for a particular month of the year or for a particular season is calculated simply as the ratio of the number of S-LLJ wind profiles to the total number of available wind profiles for that month or season over the entire 21-year study period. Similarly, the mean jet speed and jet height are calculated by averaging the LLJ speed and the LLJ height using all S-LLJ wind profiles for a particular month or season over the 21-year period. The same procedures are used to calculate the climatological values for the rawinsonde locations, although the number of available soundings is somewhat smaller because of missing observations or erroneous measurements. Most rawinsonde stations have over 90% useable soundings, with the lowest percentage just over 70%. Generally, the warm season has more useable soundings compared to the cold season, while 00 UTC has more useable soundings than 12 UTC.

The calculations are carried out at each RCM grid point and rawinsonde location and the spatial distribution of jet frequency and average jet height and speed are shown in 4-panel figures with sounding results overlaid on the RCM results. The color scale for observations and RCM model simulations are identical for better visual comparison. Pearson's Chi-squared test is used to evaluate whether the RCM-simulated S-LLJ frequencies are significantly different from observed frequencies, and Welch's unequal variance t-test is used to determine whether the simulated jet heights and speeds are

significantly different from observations. The significance testing is performed separately for each rawinsonde location using the RCM-simulated values from the nearest model grid point. In addition, the monthly S-LLJ distribution at the rawinsonde stations and the RCM grid points nearest each station are used to compare the annual cycle of S-LLJ. The annual cycles are displayed on cross-sectional plots, with the stations generally grouped from west to east and from north to south for visual comparison.

3. Results

3.1 Jet Frequency

3.1.1 Cold season S-LLJ frequencies

At 00 UTC during the cold season (October – March) (Figure 2), the observed jet frequency for the 21-year evaluation period ranges from approximately 0-14%, which broadly is the range of the RCM simulations. Higher observed frequencies are found over the southern and central plains, with the highest value (14%) at the southernmost rawinsonde station (Brownsville, Texas (BRO)), followed by 7-8% at other stations in Texas and in Oklahoma, Kansas, and eastern Nebraska. The RCM simulations generally capture the observed spatial distribution as well as the magnitude. The WRF3 and HRM3

simulations, and to a lesser extent the CRCM simulation, display weak (6-9%) frequency maxima in the central plains (Kansas, Oklahoma, and Missouri), similar to the observed pattern, whereas relatively uniform frequencies of <6% are observed over the northern and central plains and the Midwest for the RCM3 model. The higher observed jet frequencies at Corpus Christi (CRP) and BRO are missed by the model simulations except for HRM3, although the HRM3 estimates of 9-12% are somewhat lower than the observed values. In contrast, RCM3 places somewhat higher frequencies of 6-9% to the west of BRO in northeastern Mexico.

Comparisons between the S-LLJ frequencies at the rawinsonde locations with the simulated frequencies at the nearest RCM grid points provide further insights on the magnitude and significance of the deviations between simulated and observed values. When averaged over all the rawinsonde locations, the RCMs together underestimate the cool season S-LLJ frequency at 00Z by -1.6%, with the largest average deviation (-2.6%) for CRCM and the smallest (-0.9%) for WRFG (Table 1). In spite of these relatively small mean differences, the deviations between observed and simulated frequencies are statistically significant at most rawinsonde locations, in part a function of the large sample size. (Note that stations with statistically significant differences are shown as open circles in Figure 2.) HRM3 has the smallest number of locations (18 out of the 36 stations) with significant differences; in contrast, differences are significant at all but

three of the rawinsonde locations for CRCM.

The RCM simulations capture the generally higher jet frequencies at 12 UTC compared to 00 UTC during the cold season (Figure 3). The largest S-LLJ frequencies at 12 UTC in the observations are found across the central and southern plains from approximately Omaha, Nebraska (OAX) to Midland, Texas (MAF), where observed frequencies range from 10-25%, and also over CRP and BRO, where the observed values are 21% and 29%, respectively. The RCM simulations reproduce the overall spatial pattern of S-LLJ frequencies, although the areal extent of the frequency maximum for the CRCM simulation is smaller than that of the observed maximum. Also, the jet frequencies, are underestimated by all of the RCM simulations, especially in Oklahoma and northern Texas where the discrepancies can exceed 10%. All four RCMs correctly place a frequency maximum over the southern tip of Texas, although again jet frequencies are underestimated. The underestimation is greatest (approximately 10-20%) for CRCM and least (approximately 5-10%) for HRM3. In addition, the maximum is displaced westward, especially for the CRCM and RCM3 simulations. The RCM3 and WRFG simulations present somewhat greater frequency values of approximately 6-9% over the western Appalachian Highlands, which generally capture the higher observed frequency (11%) at Nashville, Tennessee (BNA). All four model simulations, but most obvious in the RCM3 simulation, produce a frequency maximum in southeast Arizona

and/or northern Mexico, which falls outside the extent of the evaluation dataset. The simulated frequencies are significantly different from observations at more stations for 12 UTC compared to 00 UTC. Again, the CRCM simulation has the largest number of locations with significant differences. Regardless of model, stations with non-significant differences tend to be located in the western and northern portions of the study area where S-LLJs are less frequent. When averaged across all stations, the underestimation of S-LLJ frequency ranges from -5.8% for CRCM to -3.2% for RCM3, with an across-model average of -4.1%.

3.1.2 Warm season S-LLJ frequencies

Warm season (April – September) S-LLJ frequencies at 00 UTC are less than 10% across most of the study domain for both observations and model simulations with the exception of HRM3 (Figure 4). An area of higher jet frequencies centered on eastern Kansas and Oklahoma is evident for both HRM3 and WRFG. This frequency maximum is considerably more pronounced in the HRM3 simulation with jet frequencies exceeding 12%, which is almost twice the magnitude of observed values. HRM3 is also the only model that presents a frequency maximum at 00 UTC in southern Texas where simulated frequencies exceed 12%. A comparable maximum is not seen in the observations. The differences between the simulated and observed frequencies are significant at almost all

rawinsonde locations, although the average differences, whether calculated for individual models or across all models, are less than 2%, with three of the models (CRCM, WRF, and RCM3) on average underestimating jet frequencies and the other (HRM3) overestimating jet frequencies (Table 1). S-LLJ frequencies increase dramatically from 00 to 12 UTC during the warm season for all the RCM simulations (Figure 5). However, the spatial pattern of jet frequency, and its coherence with observations, differs considerably between RCMs. The broad area of frequent (>12%) S-LLJ occurrences from approximately South Dakota to central Texas, as simulated by WRF, agrees most closely with the observed spatial extent, whereas relatively high (>9%) jet frequencies extend farther northward and eastward than observed for HRM3 and RCM3, respectively. HRM3 best captures the area of highest observed frequencies in the central plains (Kansas, Oklahoma, northern Texas). Jet frequencies are underestimated in this area by RCM3 and WRF where differences exceed 10% at some locations. All three models simulate a separate area of high jet frequency over extreme southern Texas, although RCM3 and HRM3 overestimate the magnitude of this frequency maximum by as much as 10%. In contrast, for the CRCM simulation the higher jet frequencies are generally confined to the central plains where the observed S-LLJ frequencies are underestimated by 15% or more, particularly in Kansas, Oklahoma, and northern Texas. Additionally, this model fails to simulate a frequency maximum over extreme southern Texas, although

a weaker (24-27%) maximum is seen farther west in northeastern Mexico. The deviations between simulated and observed frequencies, when averaged across all rawinsonde locations, highlight the propensity for CRCM and WRFG to underestimate S-LLJ frequencies (average differences of -7.1% and -2.2%, respectively) and for RCM3 and HRM3 to overestimate S-LLJ frequencies (average differences of 1.3% and 2.5%, respectively) (Table 1). Differences between the simulated and observed frequencies are significant at all but two rawinsonde locations for CRCM, but a modest number of stations (i.e., 5-10 stations) with insignificant differences are found in the northern plains and the Midwest for the other models.

Intra-seasonal (i.e., monthly) plots of S-LLJ frequency at 12 UTC further highlight the differences between models during the warm season (Figure 6). Beginning with April, all four RCMs place a frequency maximum of at least 15% in central Texas with a separate maximum in extreme southern Texas, although the magnitude and spatial extent of elevated S-LLJ frequencies varies. Between-model differences increase during May. At this time the spatial extent of jet frequencies >15% is much less for CRCM than the other three RCMs. In June and July, the frequency maximum initially in central Texas shifts northward to northern Texas and Oklahoma for all models except RCM3, and a maximum over southern Texas is no longer evident for CRCM. Model differences are greatest in August when high jet frequencies of approximately 15-25% for CRCM are

confined to a relatively small area centered over Kansas. The largest (>30%) frequencies for WRFG are also found in the central plains (Kansas and northern Oklahoma), although frequencies >15% are seen over a much larger area compared to the CRCM simulation. In contrast, the frequency maximum for HRM3 remains in northern Texas and Oklahoma where S-LLJ frequencies exceed 40%, and for RCM3 the largest frequencies of approximately 30% are located in central Texas. Additionally, only RCM3 and HRM3 display a distinct "hotspot" with S-LLJ frequencies >30% over southern Texas. The RCMs are in greater agreement in September. At this time, the frequency maximum has shifted northward into Kansas for all models. Also, the spatial extent of higher (>15%) jet frequencies has shrunk. Jet frequencies >15% persist over southern Texas only for RCM3 in September.

3.1.3 Annual cycle of S-LLJ occurrence

To evaluate how well the RCM models simulated the annual cycle of jets, the percentage of S-LLJs for each month was calculated at the RCM grid point nearest each rawinsonde station as the ratio of the number of S-LLJs found in that particular month over the 21-year period to the total number of S-LLJs (all months and all years) and then compared with observations (Figure 7). Only the results for 12 UTC are shown given the

much larger frequency of jets at this hour. For the observations, the stations located over the western and central plains (left side of the figure) display a strong annual cycle with most S-LLJs occurring during the warmest part of the year from May through September, while those located farther east have more jets during spring and autumn. Visual inspection of Figure 7 suggests that the spatial variations in the annual cycle of S-LLJ occurrence as simulated by CRCM generally agree with the observed spatial patterns. The annual cycle for WRFG, RCM3, and HRM3 also diverges from a warm season maximum to spring and autumn maxima along a west to east transect, but the shift is not as obvious as in CRCM or in the observations and occurs considerably farther east toward the Great Lakes and Appalachian Highlands. Differences also exist between stations located north and south, which is particularly obvious in the CRCM, WRFG, and HRM3 simulations. For stations in the Great Plains (station 6 to station 25), those located farther south tend to have higher S-LLJ frequencies earlier in the year than those located farther north. Furthermore, the simulations have generally darker shades of red during the warm season compared to the observations, indicating a general overestimation of the strength of the annual cycle. Additionally, the WRFG simulation generated higher percentages of jets during the winter months for stations located along the easternmost boundary of the study region, compared to the other simulations and to observations.

The differences between the model simulations and observations highlight the times

of the year with positive and negative biases in the distribution of S-LLJs at 12 UTC (Figure 8). In general, the RCMs tend to underestimate S-LLJ distribution during the cold season months and to overestimate the distribution during the warm season months. Overall, the stations located in a narrow zone from north to south in the Great Plains (stations 6-17) seem to have smaller differences compared to other stations located farther east, as indicated by the lighter shades on the left side of Figure 8 compared to the darker colors on the right side. The somewhat random discrepancies at the westernmost locations (stations 1-5) are probably due the lower total number of jets at these locations.

Monthly deviations of S-LLJ distribution, averaged across all rawinsonde locations, provide further insights on model differences in the simulated annual cycle of jets compared to observations (Table 2). The propensity of RCMs to underestimate S-LLJ distribution at 12Z during in the cold season and overestimate the warm season distribution is confirmed in Table 2 by the predominance of negative deviations for the cold season months and positive deviations in the warm season months, although considerable month-to-month differences are evident. Particularly large overestimates of S-LLJ distribution are seen for HRM3 and RCM3 during June through August, with deviations in monthly distribution ranging between 1.8-5.9%. Consequently, the annual cycle of S-LLJ is considerably too pronounced in these models. On the other hand, the largest underestimates of S-LLJ distribution are seen during October and December for

WRFG when the model frequencies fall below observed values by 3.3% and 4.3%, respectively, when averaged across rawinsonde stations. The sum of the absolute values of the monthly deviations suggests that CRCM best simulates the magnitude of the annual cycle of S-LLJs.

3.2 Jet Height

At 00 UTC during the cold season, the observed elevations of S-LLJs are higher above the ground level (AGL) over the central plains and the Gulf States (Figure 9). The highest observed values of as much as 1500 m AGL are found in Arkansas, northern Louisiana and Alabama, which is followed by stations along the Gulf Coast that have average jet heights around 1100 m AGL. In contrast, the stations along the western edge of the study area have jet heights of 900 m AGL or lower. The four model simulations capture this general pattern of jet height variation. The simulations are closer to observations at locations where jet heights are lower. This might be related to the vertical resolutions (25 mb, \sim 250 m) of the archived model outputs that are much coarser compared to the rawinsonde observations, especially farther away from the ground level. The four simulations generally underestimate, by several hundred meters in some locations, the average jet heights in the southeastern portion of the study area, but are

closer to the observations farther west. Regardless of model, the differences in observed jet elevation and the simulated elevations at the grid point nearest the rawinsonde location are significant at the majority of stations, with non-significant differences primarily confined to stations in the high plains. In general, the CRCM simulation is in closer agreement with the observations, with a mean deviation, when averaged over all rawinsonde locations, of -112 m (Table 3). Underestimation of jet elevation is considerably larger for the other three models with the greatest mean deviation (-249m) found for HRM3.

The observed average jet heights are lower at 12 UTC during the cold season, with the highest values of 900-1000 m AGL found along the Gulf of Mexico, and a decrease to around 600-800 m AGL over the western portion of the study area (Figure 10). Compared to 00 UTC, the model simulations show a similar spatial pattern at 12 UTC, but with lower jet heights. The diurnal variation in average jet height is more pronounced in the observations for the Gulf region than in the model simulations, which can be attributed to the underestimation of jet heights at 00 UTC.

The deviations between simulated and observed jet elevations when averaged across all rawinsonde locations are much smaller than for 00Z, ranging from an overestimation of jet heights of 84 m for CRCM and underestimation of 93 m for RCM3. The spatial distribution of stations with non-significant differences is less spatially coherent than at

00Z and varies between models. Differences in jet elevation are not significant at almost half of the rawinsonde locations for CRCM, whereas for RCM3 differences are not significant at only five locations.

Similar spatial patterns are observed in the warm season. However, the average warm-season jet heights are generally above 1000 m at 00 UTC (Figure 11), which is somewhat elevated from the cold-season 00 UTC jet heights. On the other hand, the heights at 12 UTC are generally within 400-800 m AGL except for stations along the Gulf Coast or in Ohio and Michigan's Lower Peninsula (Figure 12). At 00 UTC, the RCM3 simulation generally has the highest heights while the HRM3 run has the lowest. Mean deviations bear this out with, on average, RCM3 overestimating 00Z warm season jet elevations by 50 meters and HRM3 underestimating jet elevations by more than -300 m (Table 3). On the other hand, at 12Z RCM3 underestimates jet elevations (mean deviation of -77 m), whereas HRM3 overestimates jet elevations (mean deviation of 22 m). With the exception of RCM3, mean deviation in jet elevation are considerably smaller at 12Z than 00Z. Furthermore, the diurnal fluctuation in jet elevation is better simulated by the models for the warm season than during the cold season.

3.3 Jet Speed

During the cold season, the observed average S-LLJ speed reached 20 ms^{-1} in the central plains and the Midwest (Figures 13 and 14). For both 00 UTC and 12 UTC, the four models show similar spatial patterns of average jet speed with the highest speeds over the Midwest and a gradual decrease westward and southwestward, which resembles the observed spatial pattern. The diurnal variation in jet speed is modest during the cold season for both the observations and simulations. HRM3 simulates lower-than-observed jet speeds at both 00Z and 12Z, with an average underestimation of close to 2 ms^{-1} (Table 4), whereas for the other three models the average deviations is less than 1 ms^{-1} (overestimation for RCM3 and underestimation for CRCM and WRFG). The t-tests results suggest that simulated jet speeds do not differ significantly from observed values at locations from approximately the Dakotas to central Texas, with the exception of HRM3 for which significant differences are seen at almost all rawinsonde location.

The warm-season average jet speed is generally $2\text{-}4 \text{ m}^{-1}$ slower than the cold season average (Figure 15 and 16). The highest observed average jet speeds are found in the northern plains and the Midwest, with somewhat lower average speeds in the Gulf states. The four models again simulate similar spatial patterns, although RCM3 has a larger area of higher average speed compared to the other models. The diurnal variation for the warm season is also modest but slightly stronger than the cold season. For both 00 UTC and 12 UTC, the simulated values are quite close to the observations with mean differences of

less than 1 ms^{-1} for all models except HRM3. RCM3 is the only model that has positive differences (overestimation of jet speed) across the 36 stations for both 00Z and 12Z.

4. Discussion

Only a modest number of previous studies have explicitly evaluated the ability of RCMs to simulate the characteristics of S-LLJs in the central United States, even though S-LLJs are an important component of the regional climatology. Previous analyses that focused on the climatological characteristics of S-LLJs as simulated by RCMs have for the most part been limited to an evaluation of wind vectors on constant (typically 850 hPa) pressure surfaces (e.g., Cerezo-Mota *et al.*, 2011), whereas comparisons that considered the vertical wind shear profile have largely been restricted to case studies of jet events (e.g., Vanderwende *et al.*, 2015). The model evaluations presented here considerably expand on these previous analyses, as S-LLJs are identified from the vertical wind profiles of 21-year simulations from four RCMs, using criteria similar to those employed in numerous observational studies and considering both jet speed and vertical shear. This evaluation has particular significance in that the RCM simulations are from the NARCCAP suite of RCM runs that have been widely used in climate impacts studies (Mearns *et al.*, 2015). Thus, the evaluation helps to support the use of these simulations in climate assessments.

An important consideration for any model evaluation is the choice of dataset for comparison. Reanalysis datasets are often used for model evaluation (e.g., Cerezo-Mota *et al.*, 2011), in part because of the greater spatial and temporal coverage of these gridded datasets compared to observations. However, the underlying data assimilation system and forecast model, along with the resolution at which the reanalysis data are archived, can introduce biases (e.g., Mo *et al.*, 2005; Walters *et al.*, 2014). For this reason, we elected to use an observational dataset for comparison. Rawinsonde measurements are the only feasible observational dataset because of their greater spatial coverage and longer period of record compared to alternative sources (e.g., the recently discontinued NOAA Profiler Network), although their coarse temporal (twice daily) and spatial (~300 km) resolutions limit the comparisons that can be made. Inhomogeneities can also exist in the rawinsonde record due to changes during the period of record in instrumentation and observation protocols (Winkler, 2004; Walters *et al.*, 2014). The evaluations presented above highlight that, in spite of these limitations, the use of rawinsonde observations as a source of comparison provides helpful insights that can complement and supplement comparisons with reanalysis datasets.

In general, the four RCM simulations capture the characteristics of the observed S-LLJ climatology. The simulations are in good agreement with the observations when the jet frequency is low (during the cold season and at 00 UTC during the warm season),

but tend to underestimate the jet frequency when the observed values are relatively high (at 12 UTC during the warm season). Within the ensemble, the CRCM model simulated smallest jet frequency, while the HRM3 simulated largest frequencies in most cases. All simulations displayed higher jet frequencies at 12 UTC and stronger diurnal variation during the warm season, which agree with the rawinsonde observations, and are further supported by previous studies (Bonner, 1968; Mitchell *et al.*, 1995; Whiteman *et al.*, 1997). The model simulations reproduced the decrease in S-LLJ mean elevation from south-southeast to north-northwest across the study area, the higher jet elevations at 00 UTC compared to 12 UTC, and the somewhat stronger diurnal variation in jet elevation during the warm season. The simulations also captured the observed westward decrease in jet speed from the Great Lakes to the High Plains and the stronger jet speeds during the cold season compared to the warm season, with CRCM and RCM3 showing somewhat higher jet speed than WRF and HRM3.

Differences exist between the model simulations, however, with the most intriguing being the spatial placement and migration of the locations with highest jet frequencies. Dating to the early climatological analyses of Bonner (1968), the "spatial core" of warm season nocturnal S-LLJ activity has commonly been considered to be centered in Oklahoma and Kansas (Vanderwende *et al.*, 2015). Later climatological analyses employing a variety of data sources, including profiler measurements (Mitchell *et al.*,

1995), NCEP-NCAR reanalysis (Anderson and Arritt, 2001) and rawinsonde observations (Walters *et al.*, 2008), suggested a more southward location of the frequency maximum in northern Texas. More recently, Doubler *et al.* (2015), based on their climatological analysis for 1979-2009 of the 32-km resolution NARR dataset, argued for distinct centers of greater warm season nocturnal S-LLJ activity in the central plains (Kansas/Oklahoma) and in central Texas. The simulated warm season climatological patterns for the four NARCCAP RCMs suggest that, overall, nocturnal S-LLJs are most frequent in central and northern Texas, similar to recent climatological analyses, although there is a northward migration of the frequency maximum during the warm season from central Texas to Kansas/Oklahoma with the so-called "spatial core" being the primary center of jet activity only in August and September. This migration is more rapid for the CRCM simulations with S-LLJs most frequent in Kansas/Oklahoma by July, and slowest for HRCM3 with the greatest jet frequencies remaining in central Texas into August. By September all the RCMs place the frequency maximum in Kansas/Oklahoma, but a secondary maximum remains evident in northern and central Texas for all but the CRCM simulation. This migration is in general agreement with the NARR climatology (Doubler *et al.*, 2015), which suggests that nocturnal S-LLJs are most frequent in central Texas into July, with the Kansas/Oklahoma center dominant in August and September.

Model differences also exist in the simulation of the S-LLJ frequency maximum seen

over southern Texas. In the observations, this maximum is evident at 12 UTC for both the warm and cold seasons, although frequencies are considerably larger for the warm season. A similar maximum centered along the southern Texas coastline is also evident in the NARR climatology prepared by Doubler *et al.* (2015). CRCM either misses this frequency maximum entirely or underestimates its strength. In contrast, RCM3 and HRM3 overestimate the strength of this maximum, with HRM3 simulating frequent warm season S-LLJ activity in this area even at 00 UTC, which is not supported by the observations. The strength of the frequency maximum over south Texas in the RCM3 and HRM3 simulations is particularly large in July, which is later than the April-May maximum frequencies seen in the NARR climatology (Doubler *et al.*, 2015). The magnitude and timing of the south Texas maximum appears to be best captured by WRFG.

Between-model differences and deviations from observations in the spatial patterns and timing of jet occurrences may reflect differences in the relative magnitude of the forcing mechanisms responsible for S-LLJ occurrence or even unresolved processes in some RCMs compared to others. Warm season nocturnal S-LLJ occurrences in the central plains have been attributed to two boundary-layer forcing mechanisms, differential heating over the sloping terrain of the Great Plains and Rocky Mountains (Holton, 1967) and the inertial oscillation of airflow near the top of a stable nocturnal

boundary layer (Blackadar, 1957). Du and Rotunno (2014) recently argued, based on a simple 1-D analytical model, that both these mechanisms contribute to S-LLJ diurnal fluctuations during June-August in a narrow zone from southern Kansas to central Oklahoma, although Vanderwende *et al.* (2015) later demonstrated using WRF simulations of S-LLJs in Iowa that the inertial oscillation is the more important factor for locations east of largest topographic slopes. Furthermore, as shown by Vanderwende *et al.* (2015), these boundary-layer mechanisms interact with broader synoptic-scale airflow, particularly the anticyclonic airflow associated with the Atlantic subtropical high (Davis *et al.*, 1997). CRCM's focused activity in the central plains (Kansas/Oklahoma) and depressed jet frequencies may reflect weaker synoptic-scale airflow and a greater emphasis on boundary-layer forcing, whereas the southward location and higher frequencies for HRM3 and RCM3 may reflect overly strong synoptic-scale airflow. Bukovsky *et al.* (2013) provide some support for this contention, as they found the June-August 850-hPa resultant wind from Oklahoma to the western Gulf of Mexico to be much larger for HRM3 compared to the corresponding CRCM 850-hPa wind field, although this explanation is incomplete as the differences between the CRCM and RCM3 wind fields are small.

Other characteristics of the RCM simulations may also contribute to the between-model differences. For example, CRCM is the only one of the four models that

employed internal nudging extending the large-scale influence from the boundary of the RCM domain to the center of the domain (Bukovsky, 2012; Mearns *et al.*, 2012), which may partially explain the more limited spatial extent of the S-LLJ frequency maximum seen for this model and its location in the central plains. Furthermore, as raised by Bukovsky *et al.* (2013) in their evaluation of the North American monsoon, the southern boundaries of the NARCCAP simulations possibly do not extend far enough south to ensure that important larger-scale forcing translates through the model boundaries. Of particular concern is whether the model domain is sufficient to capture possible interactions between the S-LLJs and the Caribbean Jet (Cook and Vizzy, 2010), especially in southern and central Texas, and also to capture the expansion/contraction and latitudinal shifts in the airflow around the Atlantic anticyclone (Davis *et al.*, 1997).

Also of note is that the RCM simulations do not capture the annual cycle of S-LLJ frequency for locations in the eastern portion of the study area, roughly east of 93° W longitude. Here, jets are most frequent in the rawinsonde observations during spring with a secondary maximum in autumn. This timing implies that S-LLJs in the eastern portion of the study area are primarily forced by synoptic-scale mechanisms, such as strong upper-level jet streaks (Uccellini and Johnson, 1979) and developing extratropical cyclones (Carr and Millard 1985; Wu and Raman 1998), which are most frequent in the central United States during the transition seasons of spring and fall, although the

synoptically-driven jets can be enhanced by favorable boundary-layer conditions (Mitchell *et al.*, 1995; Walters, 2001). The misplacement in the RCM simulations of the annual cycle to a summer maximum at these locations suggests that the RCMs are either not capturing the synoptic-scale forcing itself or the potential boundary-layer enhancements to that forcing. Some support for the later interpretation is provided by Vanderwende *et al.* (2015), who found that the WRF model had difficulty simulating S-LLJs associated with strong frontal passages.

Generalization of the findings of this evaluation to the general ability of RCMs to simulate S-LLJs in the central United States should be undertaken cautiously. Although the NARCCAP RCMs were chosen to provide a variety of model physics (Mearns *et al.*, 2012), only a limited number of possible model configurations were considered, which often differed between models. Consequently, systematic evaluations of the influence of different parameterization schemes, horizontal and vertical resolutions, and initial and boundary conditions are not possible. Of particular note is the potential influence of the choice of global reanalysis used to drive the simulations. Comparisons by Vanderwende *et al.* (2015), for example, suggest that the choice of initial and boundary conditions has a greater influence on simulated jet occurrence than the choice of planetary boundary scheme. HRM3 appears to be particularly sensitive to boundary conditions. Mearns *et al.* (2012) found that temperature and precipitation biases for HRM3 were considerably

greater than the biases for the other NARCCAP models when this model was driven by the NCEP reanalysis, but of similar magnitude when the ERA-Interim global reanalysis was used to drive HRM3. They cautioned against over interpreting evaluations of model performance when lateral boundary conditions are supplied from only a single global reanalysis, and further argued that the quality of the reanalysis needs to be considered.

Earlier evaluations of the performance of the NARCCAP RCMs in simulating temperature and precipitation concluded that there is no best model (Mearns *et al.*, 2012). The same conclusion can be drawn from the evaluation presented here of the ability of the NARCCAP RCMs to simulate the long-term climatology of S-LLJs in the central United States. One might be tempted to rank HRM3 above the other models as the magnitude of the "hotspots" of S-LLJ frequency are generally closer to observed values, especially during the warm season, whereas the maximum jet frequencies are underestimated by the other RCMs. Some underestimation is expected, however, as the archived wind profiles from the RCMs have a coarser vertical resolution than the rawinsonde observations, limiting jet detection. The higher jet occurrences for HRM3 are more likely due to overestimation of the strength of the lower-tropospheric winds, as shown by Bukovsky *et al.* (2013). In other words, HRM3 "got the right answer for the wrong reason". On the other end of the spectrum, CRCM clearly deviates from the other models, missing the frequency maximum in southern Texas and substantially underestimating jet frequencies

elsewhere. The greatest similarity between simulations is found for WRFG and RCM3, although RCM3 overestimates S-LLJ occurrences in south Texas compared to WRFG.

The analyses presented above are only an initial step in evaluating the ability of RCMs to simulate the long-term climatology of S-LLJs in the central United States and in assessing the performance of these models for projecting future changes in jet occurrences. Important next steps include detailed examinations of the differences between models in the mechanisms contributing to jet formation. Also, further work is needed to evaluate the simulated jet climatology when the boundary conditions for the RCMs are obtained from GCM simulations for the current climate.

5. Summary

The goal of this study is to evaluate whether RCMs can simulate the long-term climatology of S-LLJs. Specifically, NARCCAP current climate simulations from four RCMs (CRCM, WRFG, RCM3, and HRM3) driven by NCEP are utilized to derive for each model a 21-year climatology of S-LLJs, and the results are compared to the observed S-LLJ climatology obtained from rawinsonde soundings in the central United States.

All four models reproduce the overall spatial patterns of S-LLJ frequency and average jet elevation and speed. The RCM simulations also capture the seasonal (cold and warm season) and diurnal (00 and 12 UTC) variations in jet frequency, elevation and

speed. The RCM-simulated jet frequencies are similar to observations during the cold season and at 00 UTC in the warm season, times when jets are less frequent. During the warm season, two of the RCMs (CRCM and WRFG) on average underestimate the frequency of nocturnal S-LLJs whereas the other two models (RCM3 and HRM3) overestimate jet frequencies. The RCMs realistically simulate the annual cycle of jet frequency at locations in the western and central plains where S-LLJs are most frequent from approximately May-September but poorly simulate the annual cycle for locations farther east where S-LLJs are most frequent in spring with a secondary maximum in fall. No model consistently outperforms the others in all aspects of the evaluation.

The RCM simulations support the existence in the central United States of three "hotspots" of S-LLJ activity, found in the central plains (Kansas/Oklahoma), central Texas, and south Texas. The location and seasonal and diurnal variations of these frequency maxima are in agreement with similar maximum identified in previous climatological analyses using multiple data sources including rawinsonde and profiler observations and global and regional reanalyses. Differences exist between the RCM simulations in the relative strength of the three maxima and the latitudinal migration of the highest jet frequencies. The CRCM simulation emphasizes the central plains maximum and underestimates the strength of the south Texas maximum, particularly during the warm season when this model fails to simulate a frequency "hotspot" in south

Texas. On the other hand, HRM3 overestimates jet frequencies in central and south Texas. All RCMs are in agreement that the location of most frequent nocturnal S-LLJ activity migrates northward from central Texas in April and May to the central plains (Kansas and Oklahoma) by August and September.

This evaluation of four RCM simulations from the NARCCAP suite demonstrates the ability of RCMs to generate the long-term climatology of S-LLJ in the central United States and the potential applications of RCMs in LLJ research. The use of a small ensemble of RCM simulations helps to identify model differences and assists with interpretation, particularly as none of the models examined here consistently outperforms others. Thus, the adoption of an ensemble under the conditions that observations are not available (for instance, under future climate) will help account for associated uncertainty.

The evaluation of the simulated S-LLJ climatologies lends confidence to the use of these models in climate impacts assessments. Work is currently underway to evaluate the simulated jet climatology when the boundary conditions for the RCMs are obtained from GCM simulations for the current climate, and to estimate future changes in the LLJ climatology for the central United States. Besides LLJ studies, many impact assessments require data with high temporal and spatial resolution, which is generally hard to achieve with observation networks or GCM simulations. Under such circumstances, RCM simulations would serve as a useful tool in analysis.

Acknowledgements: This research was supported by the National Science Foundation under Grants BCS-0924768 and BCS-0924816 and by the AgBio Research of the Michigan State University. Any opinions, findings, and conclusions or recommendations expressed in this material are those of the authors and do not necessarily reflect the view of the National Science Foundation.

Author Manuscript

References

- Anderson CJ, Arritt RW. 2001. Representation of summertime low-level jets in the central United States by the NCEP–NCAR Reanalysis. *Journal of Climate***14**: 234–247. doi: [http://dx.doi.org/10.1175/1520-0442\(2001\)014<0234:ROSLIJ>2.0.CO;2](http://dx.doi.org/10.1175/1520-0442(2001)014<0234:ROSLIJ>2.0.CO;2).
- Banta RM, Newsom RK, Lundquist JK, Pichugina YL, Coulter RL, Mahrt L. 2002. Nocturnal low-level jet characteristics over Kansas during CASES-99. *Boundary-Layer Meteorology* **105**: 221–252. doi: 10.1023/A:101992330866.
- Blackadar AK. 1957. Boundary layer wind maxima and their significance for the growth of nocturnal inversions. *Bulletin of the American Meteorological Society***38**: 283–290.
- Bonner WD. 1966. Case study of thunderstorm activity in relation to the low-level jet. *Monthly Weather Review* **94**: 167–178. doi: [http://dx.doi.org/10.1175/1520-0493\(1966\)094<0167:CSOTAI>2.3.CO;2](http://dx.doi.org/10.1175/1520-0493(1966)094<0167:CSOTAI>2.3.CO;2).
- Bonner WD. 1968. Climatology of the low-level jet. *Monthly Weather Review* **96**: 833–850. doi: [http://dx.doi.org/10.1175/1520-0493\(1968\)096<0833:COTLLJ>2.0.CO;2](http://dx.doi.org/10.1175/1520-0493(1968)096<0833:COTLLJ>2.0.CO;2).
- Bukovsky MS. 2012. Temperature trends in the NARCCAP regional climate models. *Journal of Climate***25**: 3985–3991. doi: <http://dx.doi.org/10.1175/JCLI-D-11-00588.1>.
- Bukovsky MS, Gochis DJ, Mearns LO. 2013. Toward assessing NARCCAP regional climate model credibility for the North American Monsoon: Current Climate simulations. *Journal of Climate***26**: 8802–8826. doi: <http://dx.doi.org/10.1175/JCLI-D-12-00538.1>.

Carr FH, Millard JP. 1985. A composite study of comma clouds and their association with severe weather over the Great Plains. *Monthly weather review* **113**: 370-387. doi:

[http://dx.doi.org/10.1175/1520-0493\(1985\)113<0370:ACSOCC>2.0.CO;2](http://dx.doi.org/10.1175/1520-0493(1985)113<0370:ACSOCC>2.0.CO;2).

Caya D, Laprise R. 1999. A semi-implicit semi-Lagrangian regional climate model: The Canadian RCM. *Monthly Weather Review* **127**: 341–362. doi:

[http://dx.doi.org/10.1175/1520-0493\(1999\)127<0341:ASISLR>2.0.CO;2](http://dx.doi.org/10.1175/1520-0493(1999)127<0341:ASISLR>2.0.CO;2).

Cerezo-Mota R, Allen M, Jones R. 2011. Mechanisms controlling precipitation in the northern portion of the North American monsoon. *Journal of Climate* **24**: 2771-2783. doi:

<http://dx.doi.org/10.1175/2011JCLI3846.1>.

Charney JJ, Bian X, Potter BE, Heilman WE. 2003. Low level jet impacts on fire evolution in the Mack Lake and other severe wildfires. *Proceedings, 5th Symposium on fire and forest meteorology*. American Meteorological Society: Boston, USA.

Cook KH, Vizy EK. 2010. Hydrodynamics of the Caribbean low-level jet and its relationship to precipitation. *Journal of Climate* **23**: 1477-1494. doi:

<http://dx.doi.org/10.1175/2009JCLI3210.1>.

Cook KH, Vizy EK, Launer ZS, Patricola CM. 2008. Springtime intensification of the Great Plains low-level jet and Midwest precipitation in GCM simulations of the twenty-first century. *Journal of Climate* **21**: 6321–6340. doi:

<http://dx.doi.org/10.1175/2008JCLI2355.1>.

Davis RE, Hayden BP, Gay DA, Phillips WL, Jones GV. 1997. The North Atlantic Subtropical Anticyclone. *Journal of Climate***10**: 728-744. doi:

[http://dx.doi.org/10.1175/1520-0442\(1997\)010<0728:TNASA>2.0.CO;2](http://dx.doi.org/10.1175/1520-0442(1997)010<0728:TNASA>2.0.CO;2).

Doubler DL, Winkler JA, Bian X, Zhong S, Walters CK. 2015. A NARR-derived climatology of southerly and northerly low-level jets over North America and coastal environs. *Journal of Applied Meteorology and Climatology*. In Press. doi:

<http://dx.doi.org/10.1175/JAMC-D-14-0311.1>.

Du Y, Rotunno R. 2014. A simple analytical model of the nocturnal low-level jet over the Great Plains of the United States. *Journal of the Atmospheric Sciences***71**: 3674-3683. doi:

<http://dx.doi.org/10.1175/JAS-D-14-0060.1>.

Ghan SJ, Bian X, Corsetti L. 1996: Simulation of the Great Plains low-level jet and associated clouds by general circulation models. *Monthly Weather Review* **124**: 1388–1408. doi: [http://dx.doi.org/10.1175/1520-0493\(1996\)124<1388:SOTGPL>2.0.CO;2](http://dx.doi.org/10.1175/1520-0493(1996)124<1388:SOTGPL>2.0.CO;2).

Grell GA, Devenyi D. 2002. A generalized approach to parameterizing convection combining ensemble and data assimilation techniques. *Geophysical Research Letters* **29**: 1693-1697. doi: 10.1029/2002gl015311.

Helfand HM, Schubert SD. 1995. Climatology of the simulated Great Plains low-level jet and its contributions to the continental moisture budget of the United States. *Journal of*

Climate **8**: 784–806.doi:

[http://dx.doi.org/10.1175/1520-0442\(1995\)008<0784:COTSGP>2.0.CO;2](http://dx.doi.org/10.1175/1520-0442(1995)008<0784:COTSGP>2.0.CO;2).

Holton JR. 1967. The diurnal boundary layer wind oscillation above sloping terrain.

*Tellus***19**: 199-205. doi: 10.1111/j.2153-3490.1967.tb01473.x.

Jones RG, Noguier M, Hassell DC, Hudson D, Wilson SS, Jenkins GJ, Mitchell JFB.

2004. Generating high resolution climate change scenarios using PRECIS. Met Office

Hadley Centre, Exeter, UK.

Kapela AF, Leftwich PW, Van Ess R. 1995. Forecasting the impacts of strong

wintertime post-cold front winds in the Northern Plains. *Weather and Forecasting* **10**:

229–44.doi: [http://dx.doi.org/10.1175/1520-0434\(1995\)010<0229:FTIOSW>2.0.CO;2](http://dx.doi.org/10.1175/1520-0434(1995)010<0229:FTIOSW>2.0.CO;2).

Kanamitsu M, Ebisuzaki W, Woollen J, Yang S-K, Hnilo JJ, Fiorino M, Potter GL. 2002.

NCEP–DOE AMIP-II Reanalysis (R-2). *Bulletin of the American Meteorological Society*

83: 1631–1643. doi: <http://dx.doi.org/10.1175/BAMS-83-11-1631>.

LapriseR, Caya D, Giguère M, Bergeron G, Côté H, Blanchet JP, Boer GJ, McFarlane N.

1998. Climate and climate change in western Canada as simulated by the Canadian

Regional Climate Model. *Atmosphere-Ocean* **36**: 119–167.doi:

[10.1080/07055900.1998.9649609](http://dx.doi.org/10.1080/07055900.1998.9649609).

Li B, Sain S, Mearns LO, Anderson HA, Kovats S, Ebi KL, Bekkedal MYV, Kanared MS, Patz JA. 2012. The impact of extreme heat on morbidity in Milwaukee, Wisconsin. *Climatic Change***110**: 959–76. doi: 10.1007/s10584-011-0120-y.

Liang XZ, Li L, Kunkel KE, Ting M, Wang JXL. 2004. Regional climate model simulation of US precipitation during 1982-2002. Part I: Annual cycle. *Journal of Climate***17**: 3510-3529. doi: [http://dx.doi.org/10.1175/1520-0442\(2004\)017<3510:RCMSOU>2.0.CO;2](http://dx.doi.org/10.1175/1520-0442(2004)017<3510:RCMSOU>2.0.CO;2).

Means LL. 1954. A study of the mean southerly wind maximum in low levels associated with a period of summer precipitation in the Middle West. *Bulletin of the American Meteorological Society***35**: 166–170.

Mearns LO, Arritt R, Biner S, Bukovsky M, Sain S, Caya D, Flory D, Gutowski W, Jones R, Moufouma-Okia W, Leung R, Qian Y, McGinnis S, McDaniel L, Nunes A, Roads J, Sloan L, Snyder M, Takle G, Laprise R. 2012. The North American Regional Climate Change Assessment Program: overview of Phase I results. *Bulletin of the American Meteorological Society* **93**: 1337-1362. doi: <http://dx.doi.org/10.1175/BAMS-D-11-00223.1>.

Mearns LO, Gutowski WJ, Jones R, Leung L, McGinnis S, Nunes AMB, Qian Y. 2009. A regional climate change assessment program for North America. *EOS* **90**: 311-312. doi: 10.1029/2009EO360002.

Mearns LO, *et al.* 2007 (updated 2014). The North American Regional Climate Change Assessment Program dataset, National Center for Atmospheric Research Earth System Grid data portal, Boulder, CO. doi:10.5065/D6RN35ST. (last accessed 29 October 2013)

Mearns LO, Lettenmaier DP, McGinnis S. 2015. Uses of Results of Regional Climate Model Experiments for Impacts and Adaptation Studies: the Example of NARCCAP. *Current Climate Change Reports* **1**: 1-9. doi: 10.1007/s40641-015-0004-8.

Mesinger F, DiMego G, Kalnay E, Mitchell K, Shafran PC, Ebisuzaki W, Jovic D, Woollen J, Rogers E, Berbery EH, Ek MB, Fan Y, Grumbine R, Higgins W, Li H, Lin Y, Manikin G, Parrish D, Shi W. 2006. North American regional reanalysis. *Bulletin of the American Meteorological Society* **87**: 343-360. doi: <http://dx.doi.org/10.1175/BAMS-87-3-343>.

Mitchell MJ, Arritt RW, Labas K. 1995. A climatology of the warm season Great Plains low-level jet using wind profiler observations. *Weather and Forecasting* **10**: 576-591. doi: [http://dx.doi.org/10.1175/1520-0434\(1995\)010<0576:ACOTWS>2.0.CO;2](http://dx.doi.org/10.1175/1520-0434(1995)010<0576:ACOTWS>2.0.CO;2).

Mo KC, Chelliah M, Carrera ML, Higgins RW, Ebisuzaki W. 2005. Atmospheric moisture transport over the United States and Mexico as evaluated in the NCEP regional reanalysis. *Journal of Hydrometeorology* **6**: 710-728. doi: <http://dx.doi.org/10.1175/JHM452.1>.

Pal JS, Giorgi F, Bi X, Elguindi N, Solmon F, Rauscher SA, Gao X, Francisco R, Zakey A, Winter J, Ashfaq M, Syed FS, Sloan LC, Bell JL, Diffenbaugh NS, Karmacharya J, Konaré A, Martinez D, da Rocha RP, Steiner AL. 2007. The ICTP RegCM3 and RegCNET: regional climate modeling for the developing world. *Bulletin of the American Meteorological Society* **88**: 1395-1409. doi: <http://dx.doi.org/10.1175/BAMS-88-9-1395>.

Pitchford KL, London J. 1962. The low-level jet as related to nocturnal thunderstorms over Midwest United States. *Journal of Applied Meteorology* **1**: 43–47. doi: [http://dx.doi.org/10.1175/1520-0450\(1962\)001<0043:TLLJAR>2.0.CO;2](http://dx.doi.org/10.1175/1520-0450(1962)001<0043:TLLJAR>2.0.CO;2).

Qiao L, Pan Z, Herrmann RB, Hong Y. 2014. Hydrological variability and uncertainty of lower Missouri river basin under changing climate. *Journal of the American Water Resources Association* **50**: 246–60. doi:10.1111/jawr.12126.

Sjostedt DW, Sigmon JT, ColucciSJ. 1990. The Carolina nocturnal low-level jet: synoptic climatology and a case study. *Weather and Forecasting* **5**: 404–415. doi: [http://dx.doi.org/10.1175/1520-0434\(1990\)005<0404:TCNLLJ>2.0.CO;2](http://dx.doi.org/10.1175/1520-0434(1990)005<0404:TCNLLJ>2.0.CO;2).

Skamarock WC, Klemp JB, Dudhia J, Gill DO, Barker DM, Wang W, Powers JG. 2005. A description of the Advanced Research WRF Version 2, NCAR Tech Notes-468+STR, National Center for Atmospheric Research, Boulder, Colorado.

Song J, Liao K, Coulter RL, Lesht BM. 2005. Climatology of the low-level jet at the southern Great Plains atmospheric boundary layer experiments site. *Journal of Applied Meteorology* **44**: 1593–606. doi: <http://dx.doi.org/10.1175/JAM2294.1>.

Stensrud DJ. 1996. Importance of low-level jets to climate: A review. *Journal of Climate* **9**: 1698–1711. doi: [http://dx.doi.org/10.1175/1520-0442\(1996\)009<1698:IOLLJT>2.0.CO;2](http://dx.doi.org/10.1175/1520-0442(1996)009<1698:IOLLJT>2.0.CO;2).

Storm B, Dudhia J, Basu S, Swift A, Giammanco I. 2009. Evaluation of the Weather Research and Forecasting model on forecasting low-level jets: implications for wind energy. *Wind Energy* **12**: 81-90. doi: 10.1002/we.v12:1.

Takle ES, Jha M, Lu E, Arritt RW, Gutowski WJ. 2010. Streamflow in the upper Mississippi river basin as simulated by SWAT driven by 20th Century contemporary results of global climate models and NARCCAP regional climate models. *Meteorologische Zeitschrift* **19**: 341-346. doi:

<http://dx.doi.org/10.1127/0941-2948/2010/0464>.

Uccellini LW, Johnson DR. 1979. Coupling of upper and lower tropospheric jet streaks and implications for the development of severe convective storms. *Monthly Weather Review* **107**: 682-703. doi:

[http://dx.doi.org/10.1175/1520-0493\(1979\)107<0682:TCOUAL>2.0.CO;2](http://dx.doi.org/10.1175/1520-0493(1979)107<0682:TCOUAL>2.0.CO;2).

Vanderwende BJ, Lundquist JK, Rhodes ME, Takle ES, Irvin SL. 2015. Observing and Simulating the Summertime Low-Level Jet in Central Iowa. *Monthly*

Weather Review **143**: 2319–2336. doi: <http://dx.doi.org/10.1175/MWR-D-14-00325.1>.

Walters CK. 2001. Airflow configurations of warm season southerly low-level wind maxima in the Great Plains. Part II: The synoptic and subsynoptic-scale environment.

Weather and Forecasting **16**: 531-551. doi:

[http://dx.doi.org/10.1175/1520-0434\(2001\)016<0531:ACOWSS>2.0.CO;2](http://dx.doi.org/10.1175/1520-0434(2001)016<0531:ACOWSS>2.0.CO;2).

Walters CK, Winkler JA, Shadbolt RP, van Ravensway J, Bierly GD. 2008. A long-term climatology of southerly and northerly low-level jets for the central United States. *Annals of the Association of American Geographers* **98**: 521-552. doi:

[10.1080/00045600802046387](http://dx.doi.org/10.1080/00045600802046387).

Walters CK, Winkler JA, Husseini S, Keeling R, Nikolic J, Zhong S. 2014. Low-level jets in the North American Regional Reanalysis (NARR): a comparison with rawinsonde observations. *Journal of Applied Meteorology and Climatology* **53**: 2093–2113. doi:

<http://dx.doi.org/10.1175/JAMC-D-13-0364.1>.

Werth D, Kurzeja R, Dias NL, Zhang G, Duarte H, Fischer M, Parker M, Leclerc M. 2011. The simulation of the southern Great Plains nocturnal boundary layer and the low-level jet with a high-resolution mesoscale atmospheric model. *Journal of Applied Meteorology and Climatology* **50**: 1497-1513. doi: <http://dx.doi.org/10.1175/2011JAMC2272.1>

Whiteman CD, Bian X, Zhong S. 1997. Low-level jet climatology from enhanced rawinsonde observations at a site in the southern Great Plains. *Journal of Applied Meteorology and Climatology* **36**:1363-1376. doi:

[http://dx.doi.org/10.1175/1520-0450\(1997\)036<1363:LLJCFE>2.0.CO;2](http://dx.doi.org/10.1175/1520-0450(1997)036<1363:LLJCFE>2.0.CO;2).

Winkler JA. 2004. The impact of technology upon in situ atmospheric observations and climate science. In *Geography and Technology*, Brunn SD, Cutter SL, Harrington Jr. JW (ed). Springer: Netherlands, 461-490.

Winkler JA, Guentchev GS, Liszewska M, Perdinan, Tan P. 2011. Climate scenario development and applications for local/regional climate change impact assessments: an overview for the non-climate scientist. *Geography Compass* **5**: 301-328. doi: 10.1111/j.1749-8198.2011.00426.x.

Wu Y, Raman S. 1998. The summertime Great Plains low level jet and the effect of its origin on moisture transport. *Boundary-Layer Meteorology* **88**: 445-466. doi: 10.1023/A:1001518302649.

Zhang H, Huang GH, Wang D, Zhang X. 2011. Uncertainty assessment of climate change impacts on the hydrology of small prairie wetlands. *Journal of Hydrology* **396**: 94-103. doi:10.1016/j.jhydrol.2010.10.037.

List of Tables

Table 1. Mean differences (in percent) between RCM simulated and observed S-LLJ frequencies, averaged for 36 rawinsonde stations for the cold (October-March) and warm (April-September) seasons. The RCM values are for the model grid point closest to the station location.

Table 2. Differences (in percent) between RCM and observed monthly distributions of S-LLJ occurrence, averaged for all 36 rawinsonde locations. The RCM values are for the model grid point closest to the station location.

Table 3. Mean differences (in meters) between RCM simulated and observed S-LLJ elevations, averaged for 36 rawinsonde stations for the cold (October-March) and warm (April-September) seasons. The RCM values are for the model grid point closest to the station location.

Table 4. Mean differences (in meters per second) between RCM simulated and observed S-LLJ speed, averaged for 36 rawinsonde stations for the cold (October-March) and warm (April-September) seasons. The RCM values are for the model grid point closest to the station location.

List of Figures

Figure 1. Study domain, the topography (shading) as resolved by the CRCM and the locations (circles) and evaluations (shading) of the 36 rawinsonde stations used in the study. Units in meters.

Figure 2. Cold-season 00 UTC RCM-simulated (shading) and rawinsonde observed (shading and number next to the station circle) jet frequency. An open circle indicates that the RCM simulated results and observations are significantly different, while a circle with a cross indicates non-significant differences. A circle with a dot indicates insufficient data for the significance tests. White shading represents locations with no S-LLJ occurrences.

Figure 3. Same as Figure 2, but for 12 UTC

Figure 4. Same as Figure 2, but for warm season

Figure 5. Same as Figure 4, but for 12 UTC

Figure 6. Jet frequency at 12 UTC during April to September for the four RCMs.

Figure 7. Percentage of jet events in each month of the year for the 36 stations. At each station, the percentages from all 12 months sum up to 100%. The x-axis represents station numbers, and the y-axis represents the 12 months of the year, numbered consecutively from January (1) to December (12). The stations numbered 1 to 36 are TFX, GGW, DNR,

ABQ, EPZ, UNR, BIS, LBF, DDC, AMA, MAF, DRT, ABR, OAX, TOP, OUN, FWD,
CRP, BRO, INL, MPX, SGF, LZK, SHV, LCH, DVN, ILX, JAN, SIL, GRB, APX, DTX,
ILN, BNA, BMX, and BUF.

Figure 8. Difference (in percent) in RCM simulated and observed jet distributions by month for the 36 stations.

Figure 9. Cold-season 00 UTC RCM-simulated (shading) and rawinsonde observed (shading and number next to the station circle) jet height. Units in meters AGL.

Figure 10. Same as Figure 9, but for 12 UTC

Figure 11. Same as Figure 9, but for warm season

Figure 12. Same as Figure 11, but for 12 UTC

Figure 13. Cold-season 00 UTC RCM-simulated (shading) and rawinsonde observed (shading and number next to the station circle) jet speed. Units in ms^{-1} .

Figure 14. Same as Figure 13, but for 12 UTC

Figure 15. Same as Figure 13, but warm season

Figure 16. Same as Figure 15, but for 12 UTC

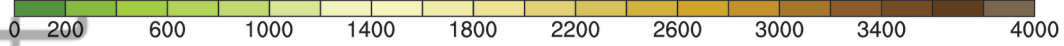
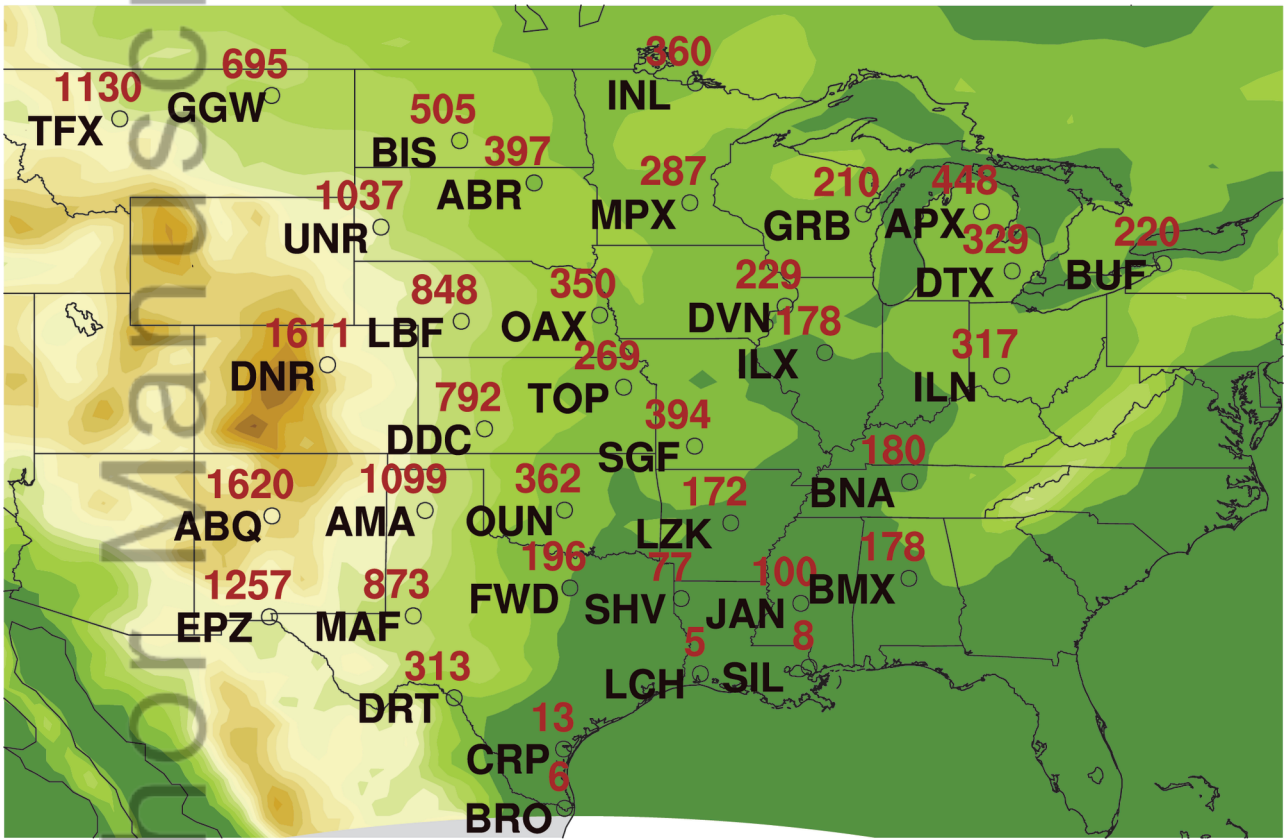


figure1

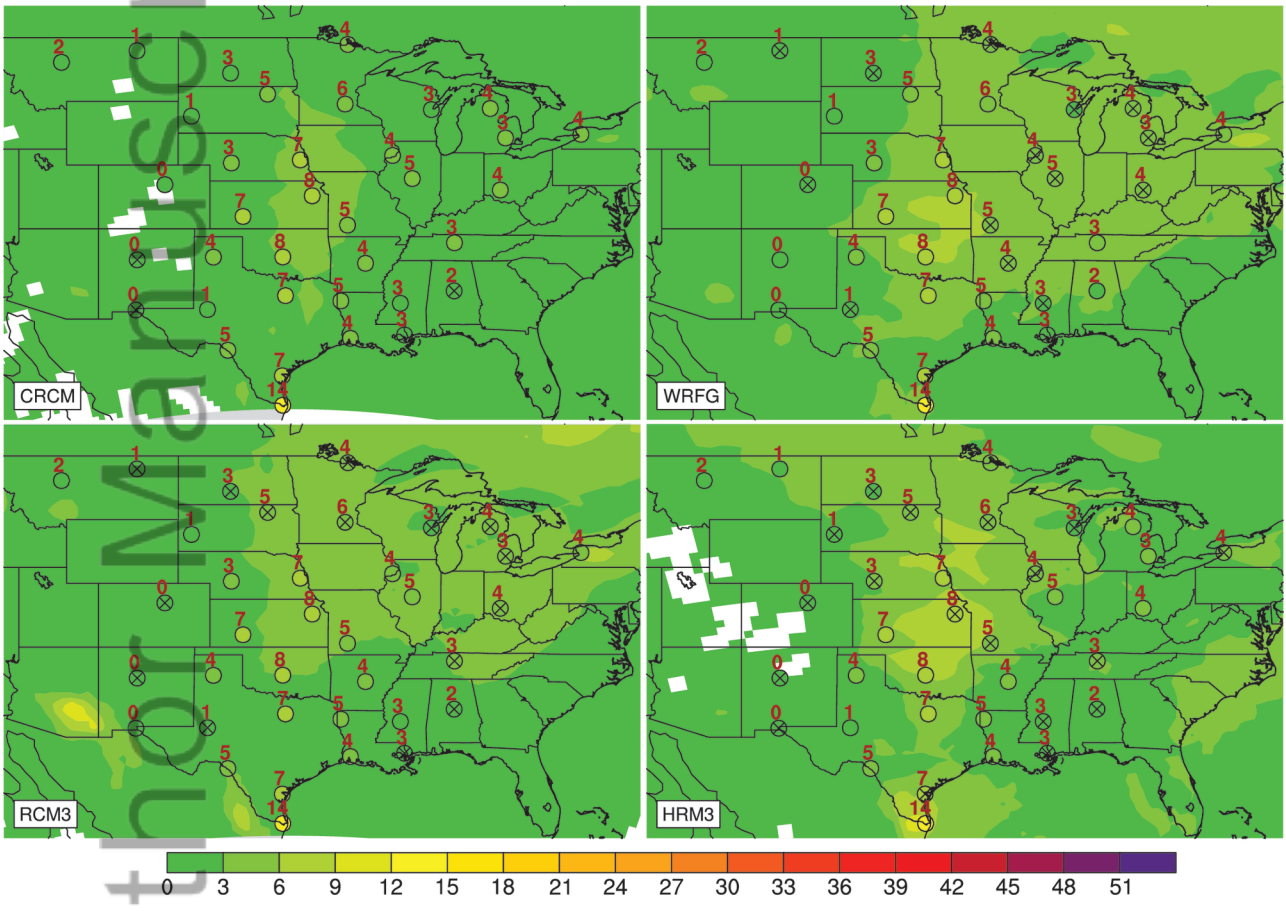


figure2

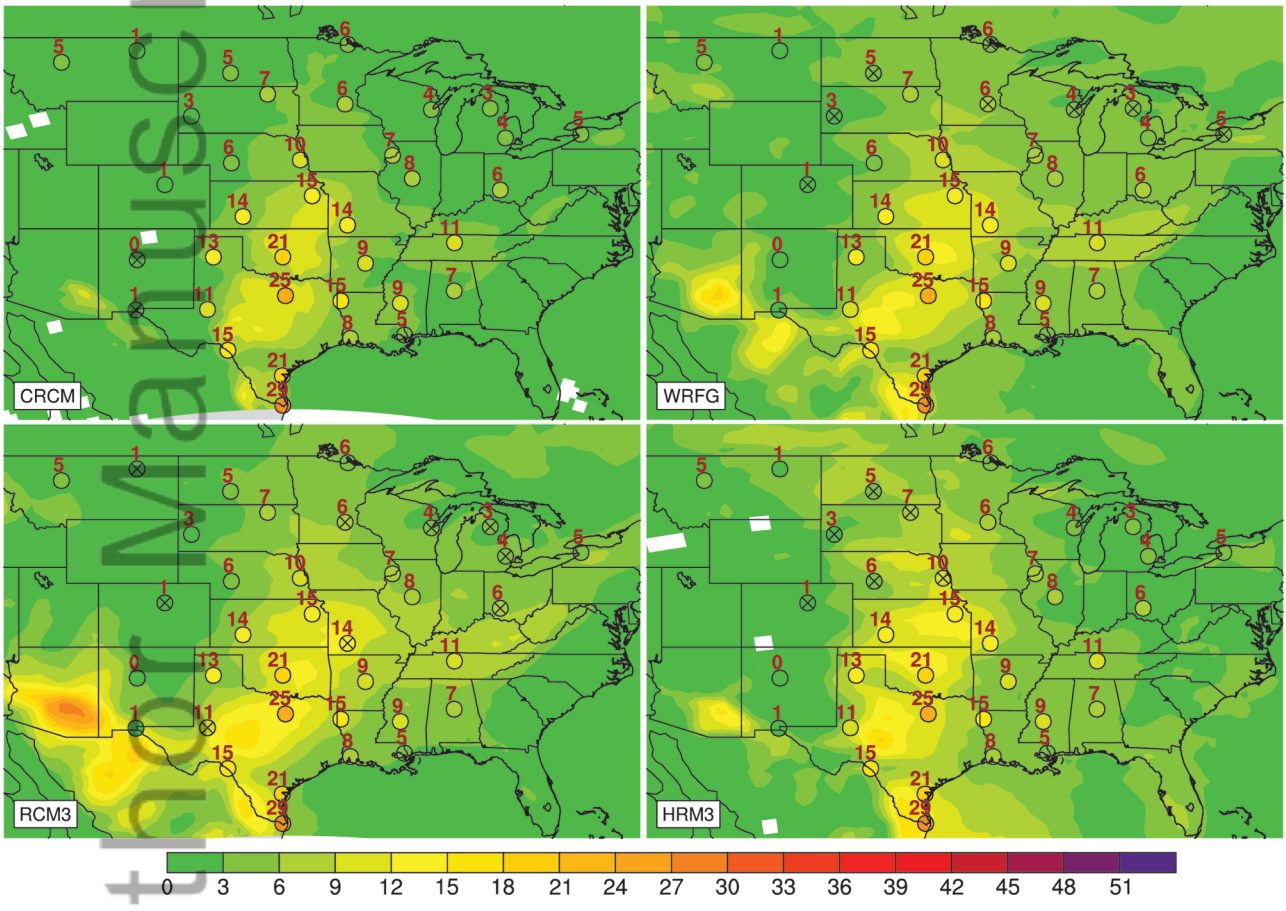


figure3

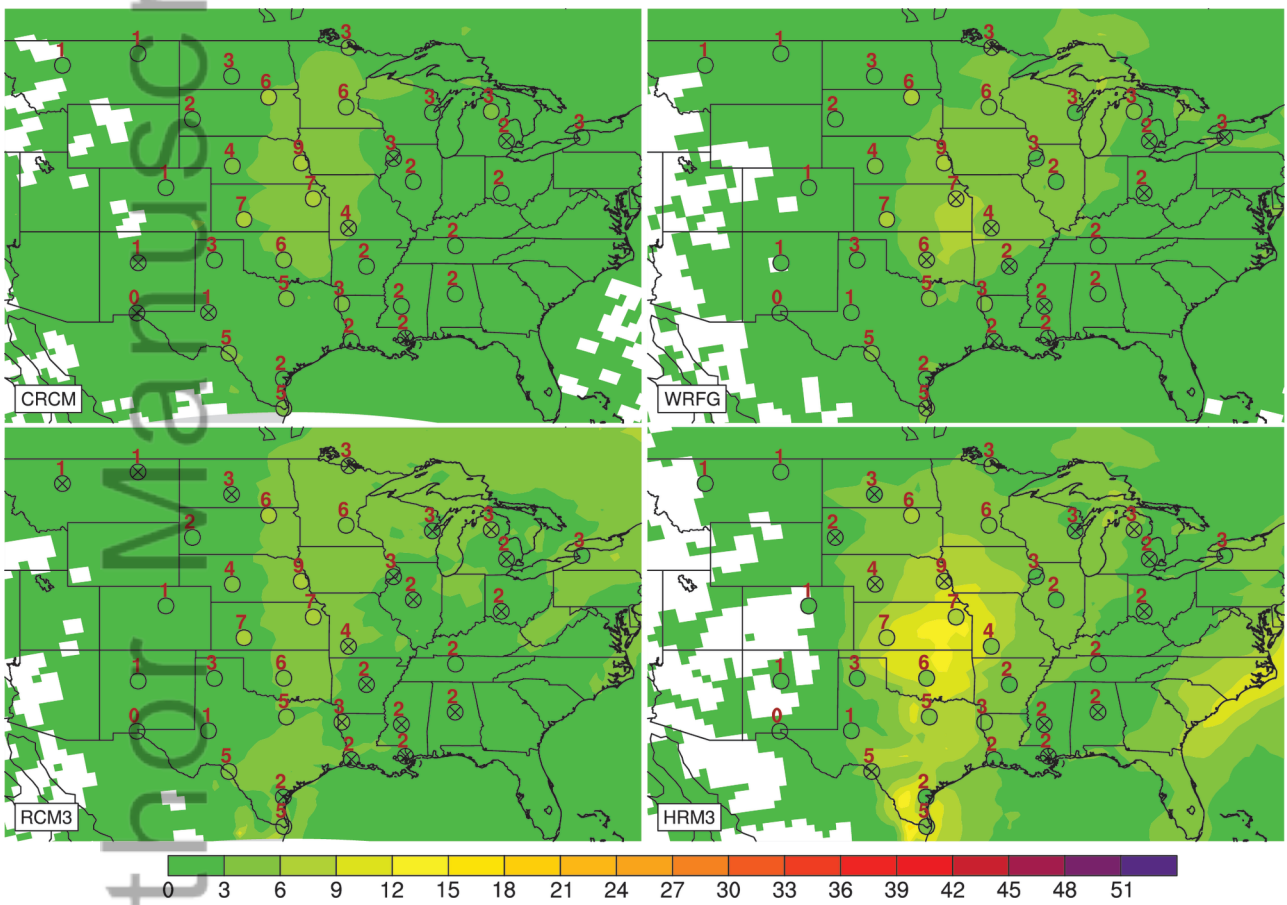


figure4

Autonomous Manuscript

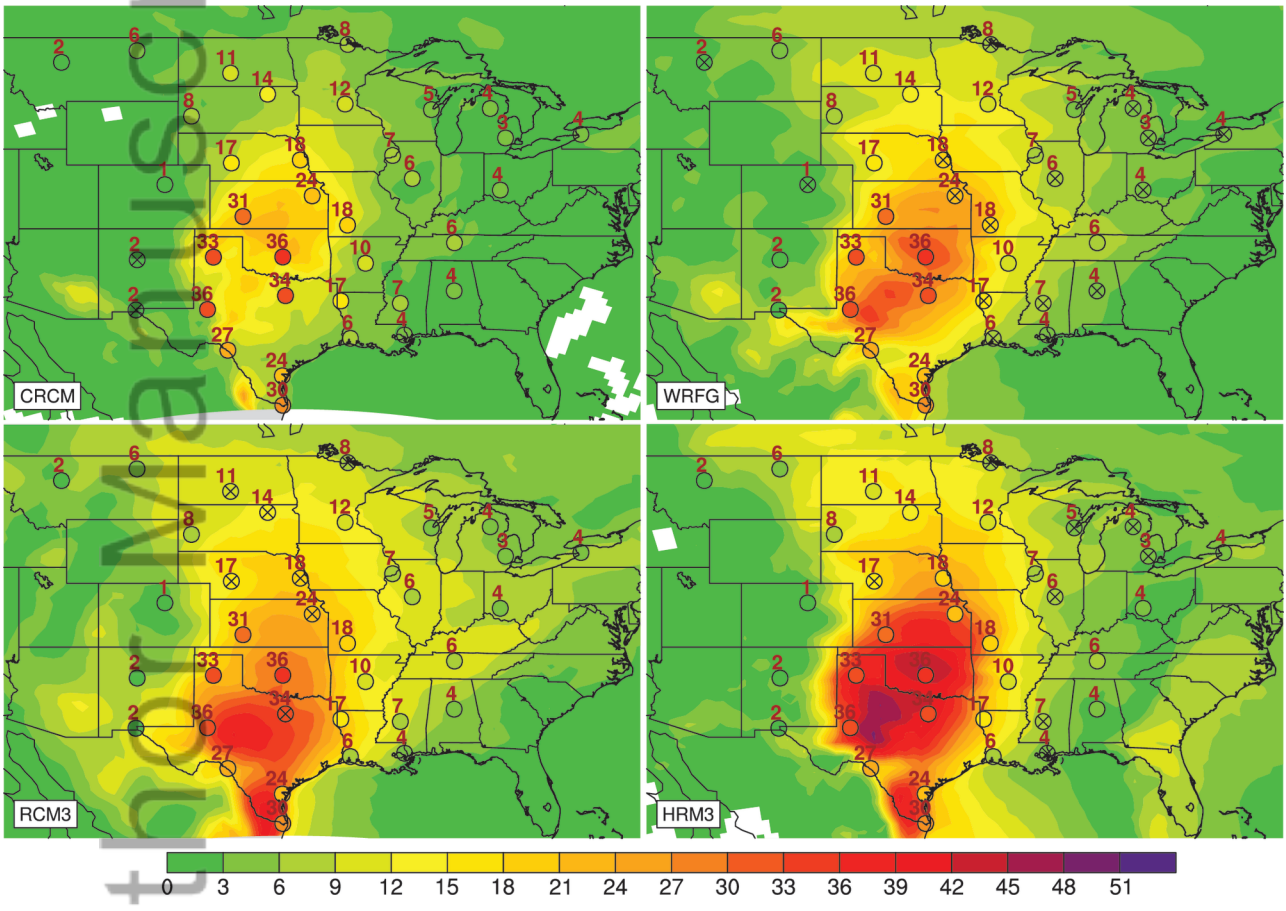


figure5

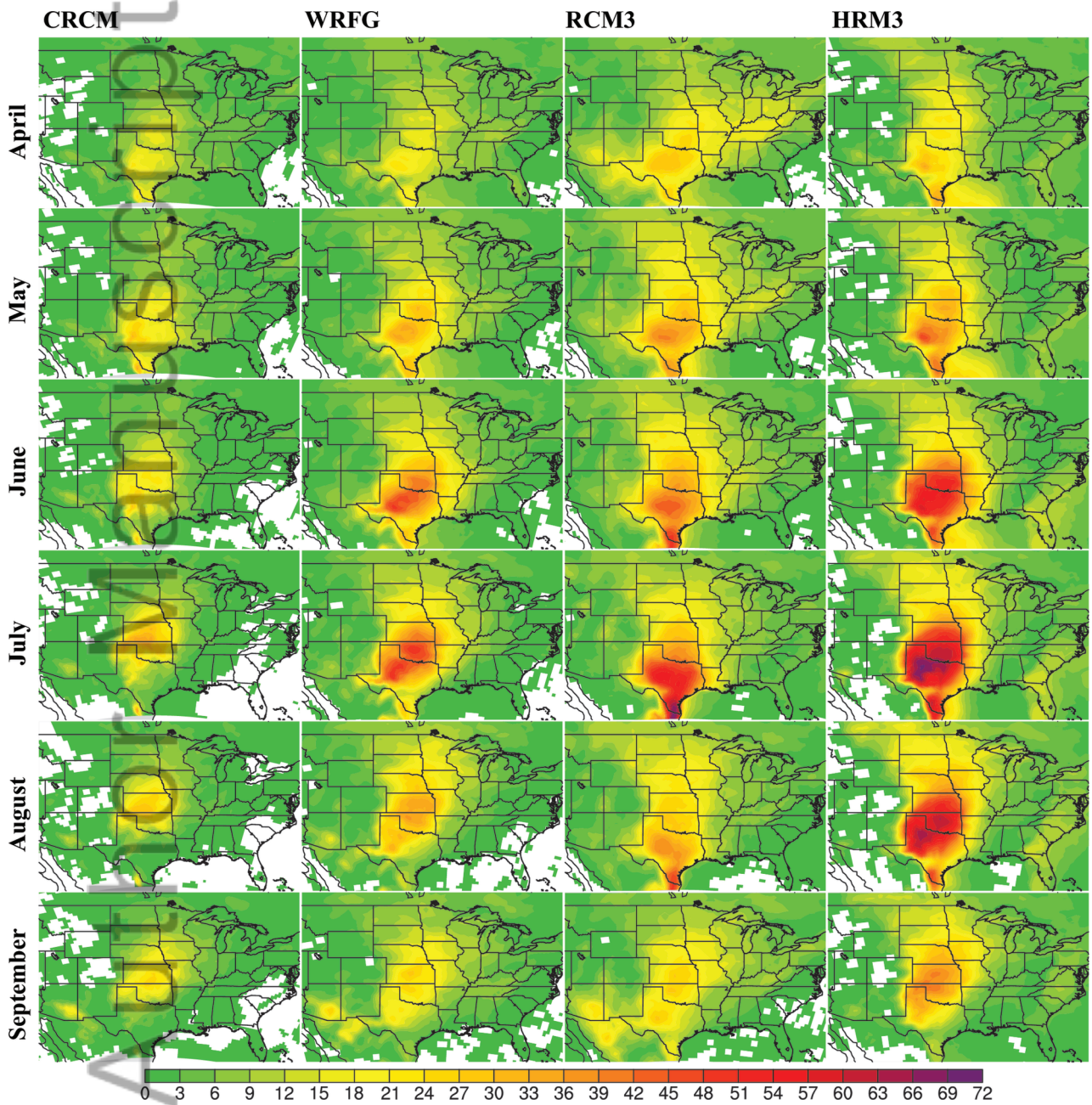


figure6

Author Manuscript

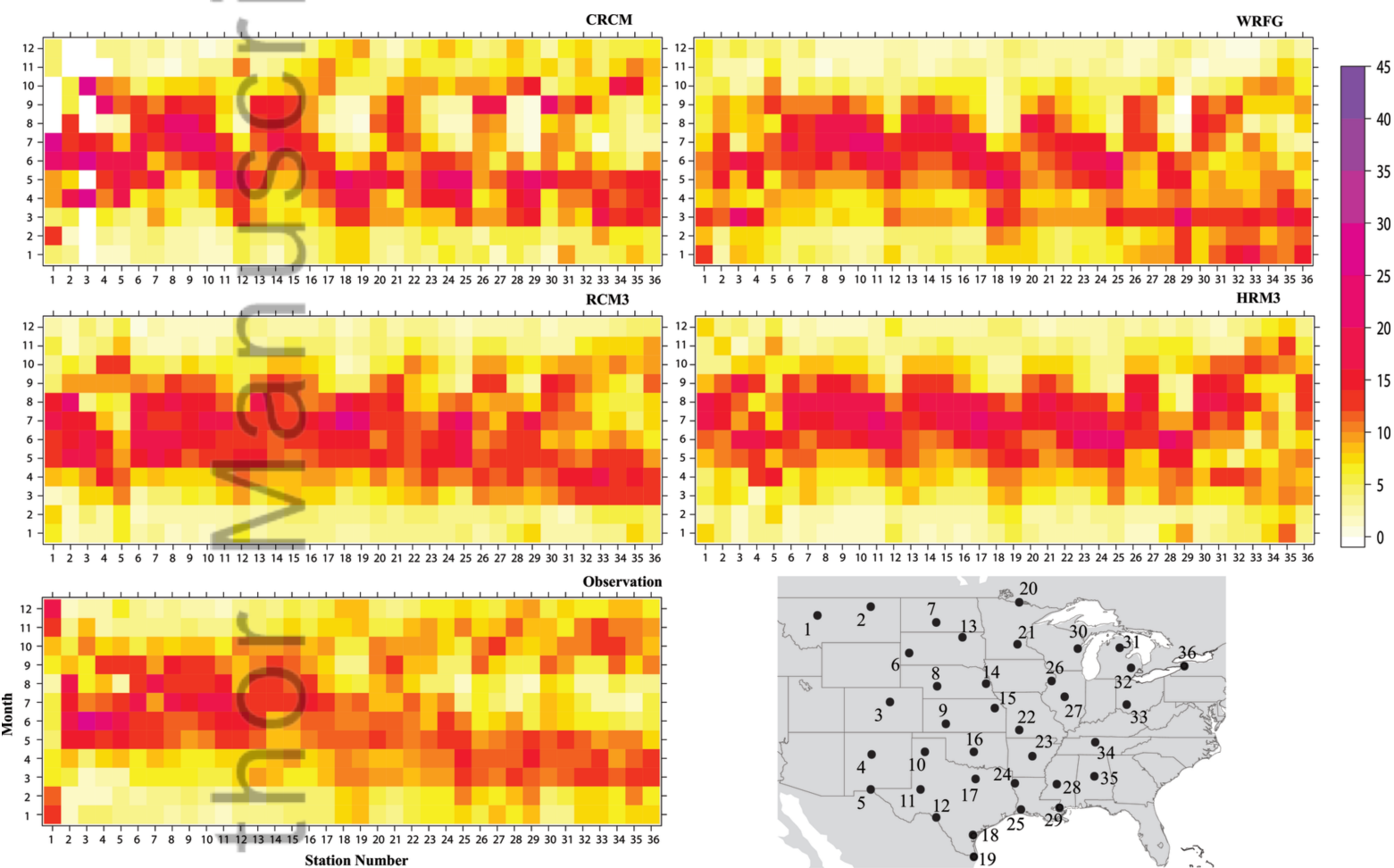


figure7

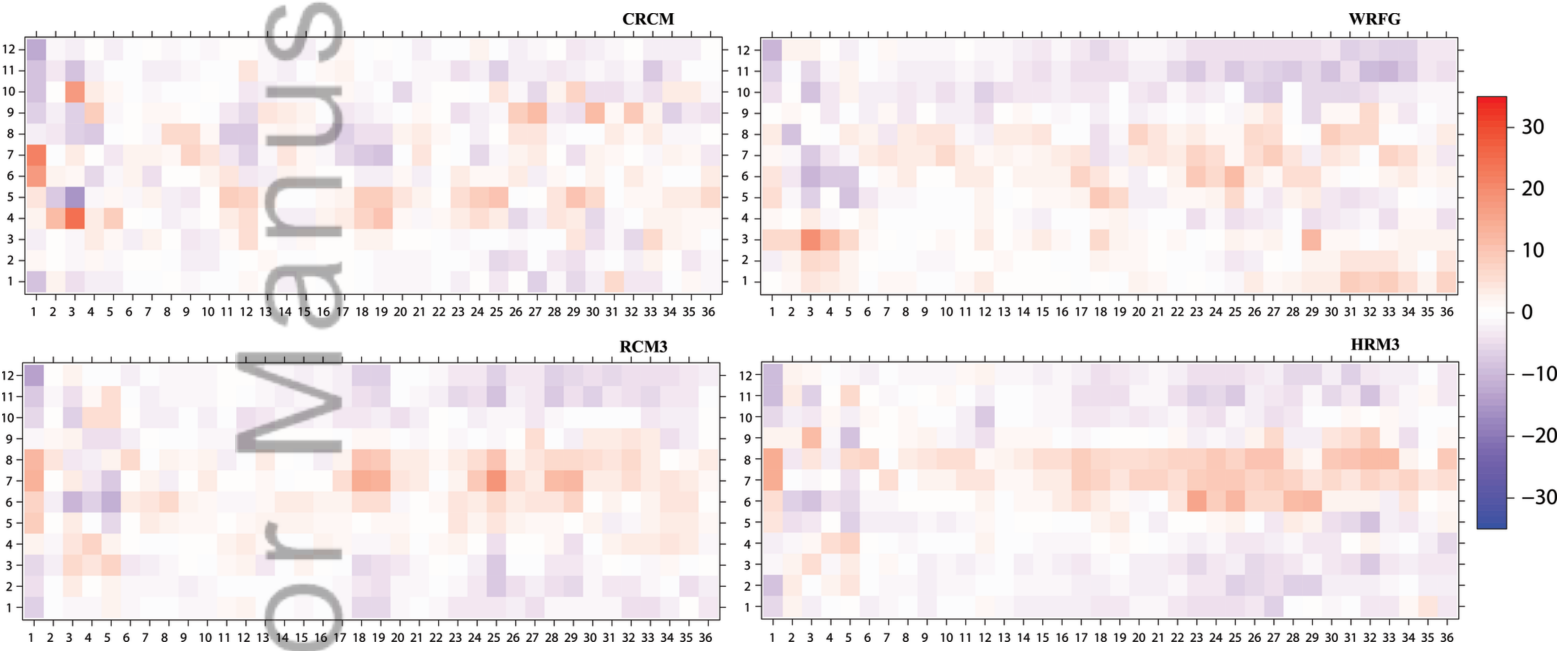


figure8

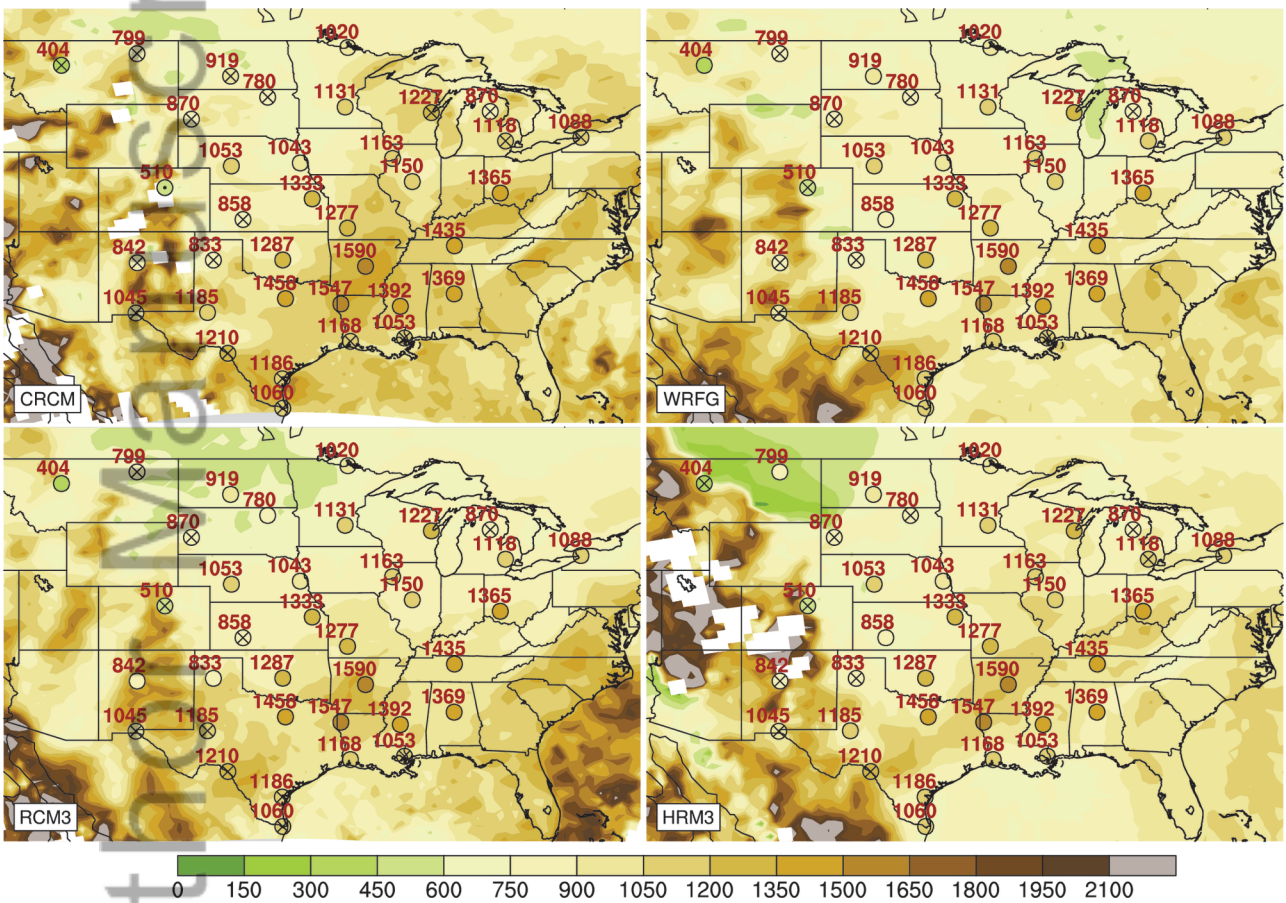


figure9

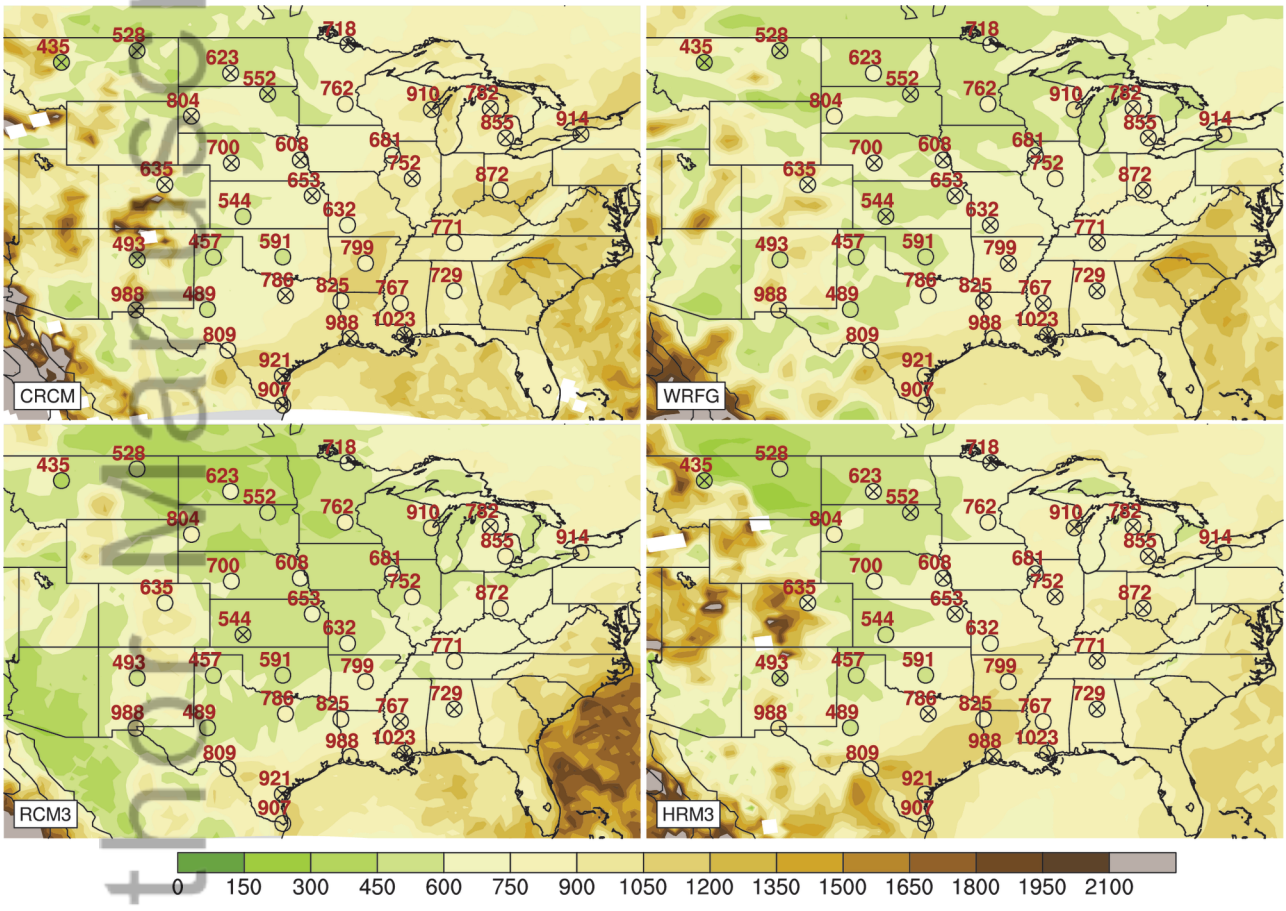


figure10

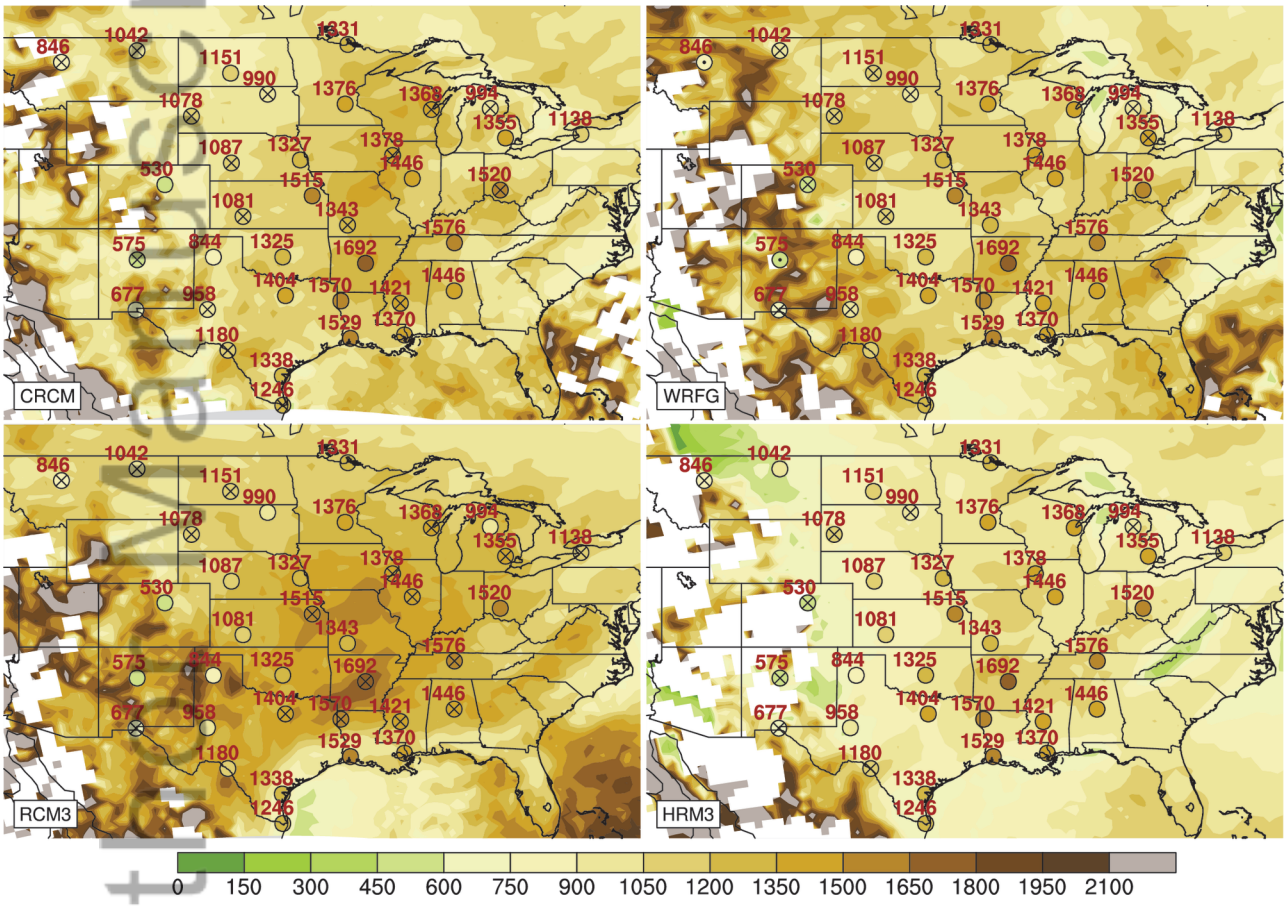


figure11

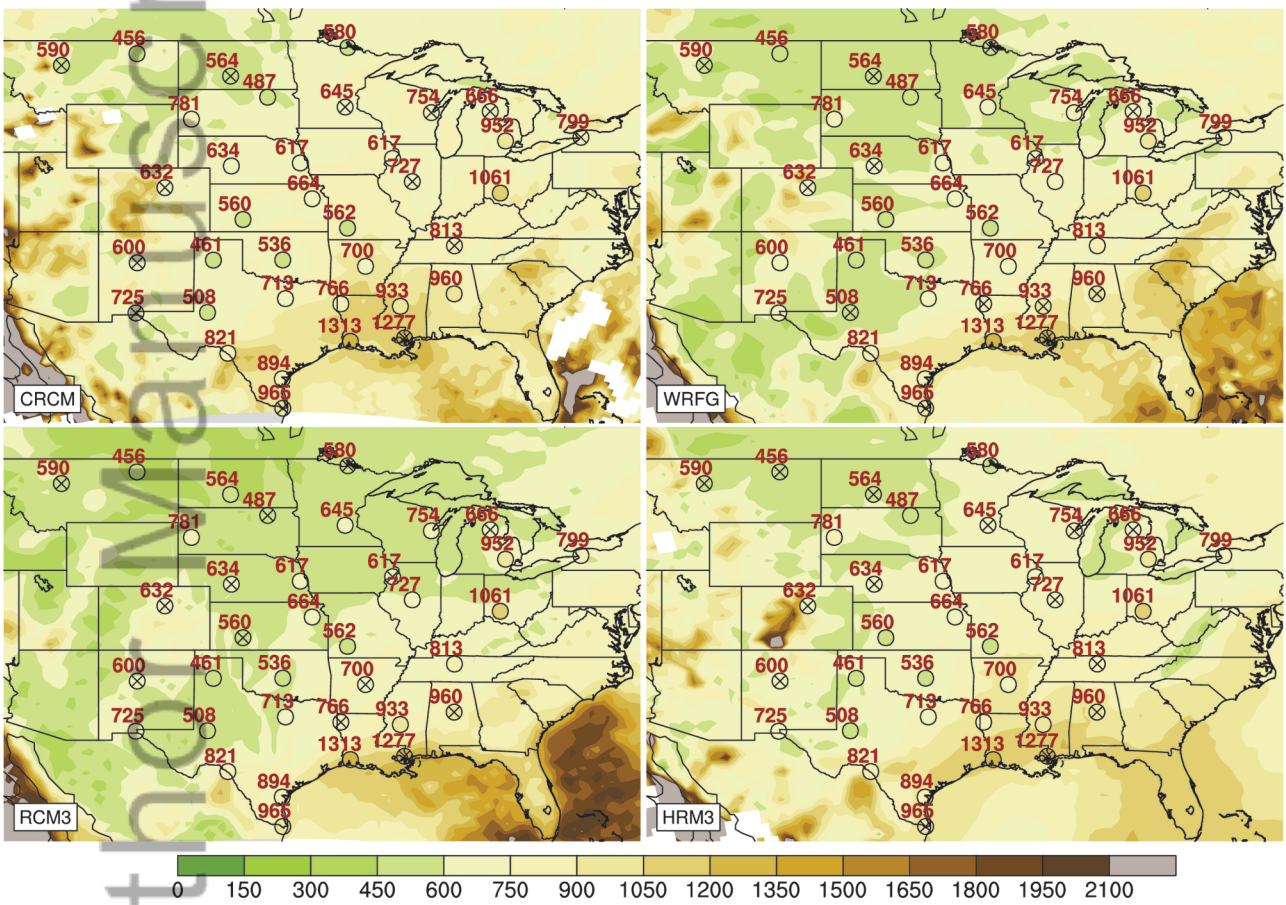


figure12

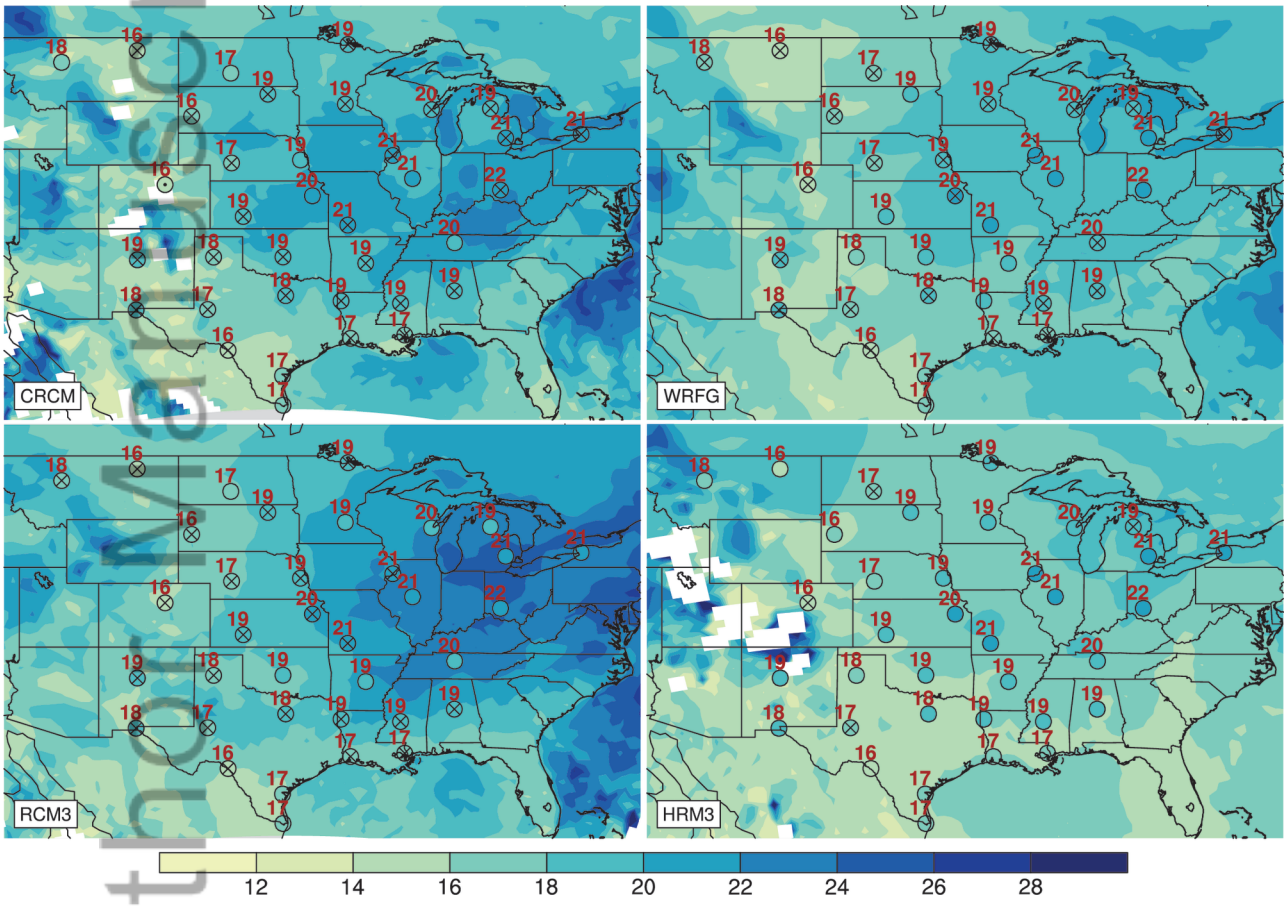


figure13

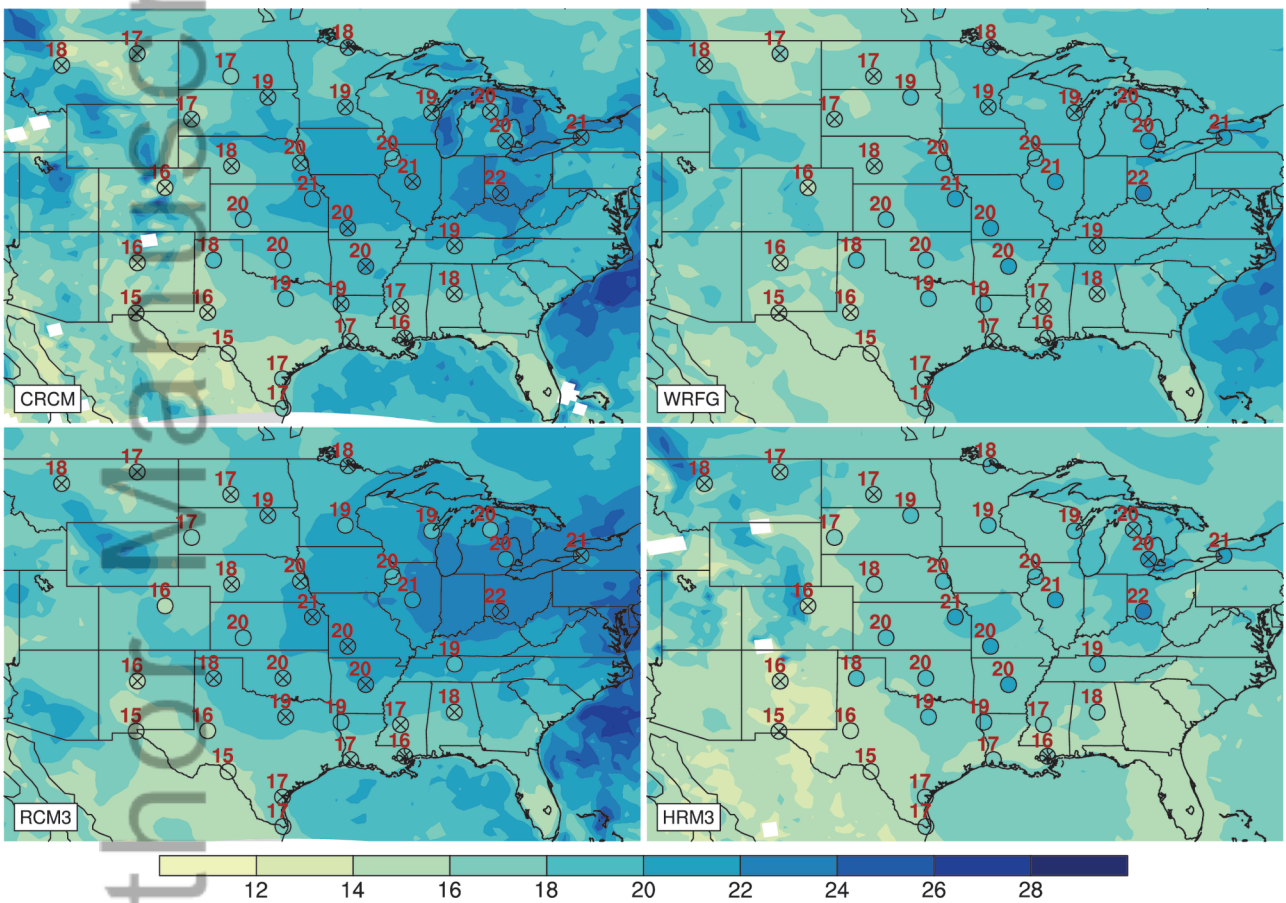


figure14

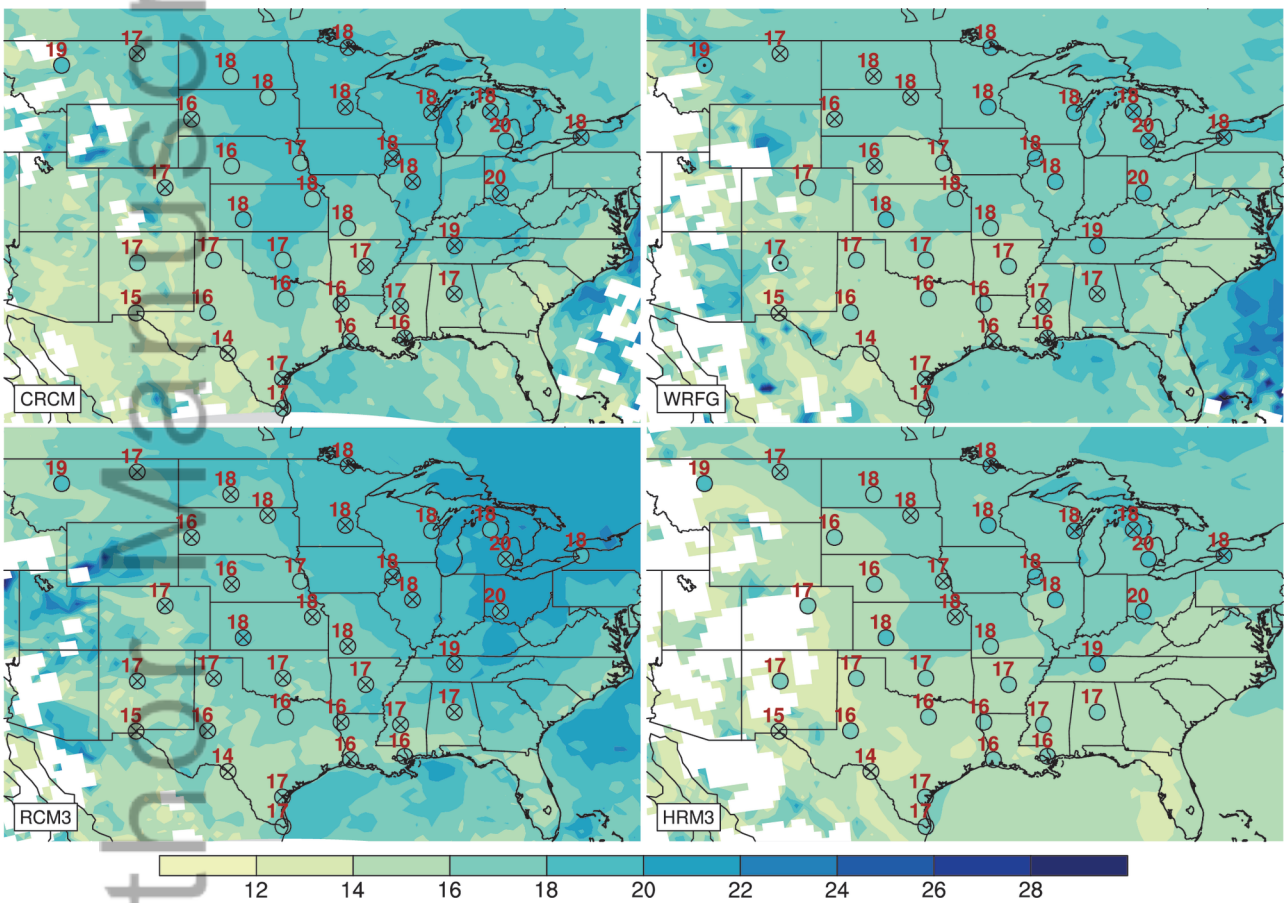


figure15

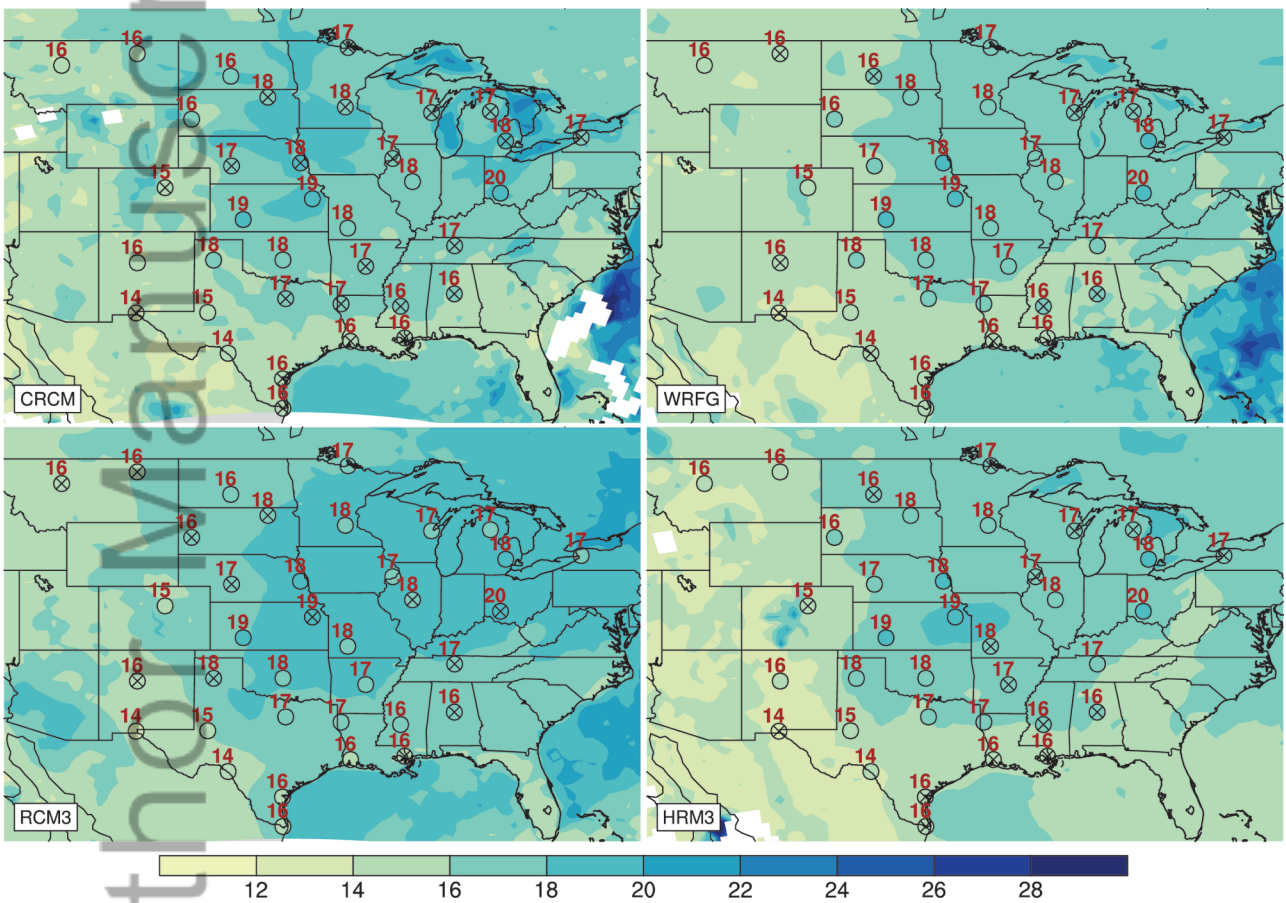


figure16